Effect of Circadian Meal Pattern on Obesity and Depressive-like Behavior in Mice

マウスの肥満やうつ様行動に対する概日性食餌パターンの影響

February 2018

Atsushi HARAGUCHI

原口 敦嗣

Effect of Circadian Meal Pattern on Obesity and Depressive-like Behavior in Mice

マウスの肥満やうつ様行動に対する概日性食餌パターンの影響

February 2018

Waseda University

Graduate School of Advanced Science and Engineering

Department of Advanced Science and Engineering,

Research on Electrical Engineering and Bioscience B

Atsushi HARAGUCHI

原口 敦嗣

Table of contents

Abbreviationd

5-HIAA; 5-hydroxyindole acetic acid

5-HT; 5-hydroxytryptamine, serotonin

ANOVA; analysis of variance

AUC; area under the blood glucose concentration time curve

Bmal1; brain and muscle arnt-like protein 1

Clock; circadian locomoter output cycles kaput

Comt; catechol-O-methyltransferase

Cry; cryptochrome

CYP7A1; cholesterol 7α-hydroxylase

EDTA; ethylenediaminetetraacetic acid

FF; free feeding

FST; forced swimming test

GLUT2; glucose transporter 2

HFD; high-fat diet

HPLC-ECD; High performance liquid chromatography-electrochemical detection

IVIS; *in vivo* imaging system

LD; light-dark

Mao; monoamine oxidase

MHPG; 3-methoxy-4-hydroxyphenylglycol

mRNA; messenger ribonucleic acid

NE; norepinephrine

NES; night eating syndrome

ND; normal-fat diet

Per; period

PER2::LUC; PERIOD2::LUCIFERASE

PEPCK; phosphoenolpyruvate carboxykinase

Rev-erb; reverse erythroblastosis virus

RF; restricted feeding

ROI; region of interest

ROR; retinoic acid receptor-related orphan receptor

RORE: ROR responsive element

SCN; suprachiasmatic nucleus

SEM; standard error of the mean

SSRIs; selective serotonin reuptake inhibitors

ZT; zeitgeber time

Chapter 1. Introduction

Almost all plants and animals on earth live under an environmental light-dark (LD) cycle, which is controlled by sunrise and sunset. Moreover, under constant dark conditions, organisms live in approximately 24 hours period, which is called circadian rhythm. Many physiological functions, such as the sleep-wake cycle, metabolism, control of body temperature and appetite, and other functions of various organs show circadian variation, and the mechanism that provides circadian fluctuation of physiological functions is called the circadian clock system (Gachon et al., 2004; Golombek & Rosenstein, 2010). The mammalian circadian clock system is composed of various clock genes. In particular, *Cryptochrome1/2* (*Cry1/2*), *Period1/2* (*Per1/2*), *Brain and muscle arnt-like protein 1* (*Bmal1*), and *Circadian locomoter output cycles kaput* (*Clock*) are the core clock genes that form the transcriptional-translational feedback loop, which produces an approximately 24-hour cycle (Bass & Takahashi, 2010; Asher & Schibler, 2011; Buhr & Takahashi, 2013). Heterodimers of CLOCK and BMAL1 (CLOCK/BMAL1), which act as transcriptional activators, activate the transcription of *Per* and *Cry* through binding to a specific promoter domain, which is called the E-box. *Per* and *Cry* mRNA move to the cytoplasm and are translated into proteins. Subsequently, they form heterodimers and move back to the nucleus. Thereafter, they decrease the transcription of *Per* and *Cry* by binding to CLOCK/BMAL1. Consequently, mRNA and protein levels of PER and CRY maintain rhythmicity throughout an approximately 24-hour period. Moreover, *Retinoic acid receptor-related orphan receptor* (*Ror*) and *Reverse erythroblastosis virus* (*Rev-erb*), which are other clock genes, generate a transcription-activating rhythm through binding to ROR

responsive element (RORE), which is another specific promoter domain (Albrecht, 2012; Mohawk et al., 2012). These feedback loops enable approximately 10% of all genes to show rhythmicity (Ueda et al., 2002; Oishi et al., 2003; Miller et al., 2007; Hughes et al., 2009), and these genes are named clock-controlled genes. These genes regulate many physiological functions, including metabolism, the maintenance of muscle, as well as monoamine synthesis and metabolism (Bailey et al., 2014; Gooley, 2016; Aoyama & Shibata, 2017; Hampp et al., 2008; Suárez-Trujillo & Casey, 2016) (Figure 1.1). For example, cholesterol 7α-hydroxylase (CYP7A1), which is a rate-limiting enzyme for bile acid synthesis, shows circadian fluctuation under the control of clock genes (Gooley, 2016). In addition, liver-specific *Bmal1* knock-out mice showed a lack of circadian rhythmicity and showed decreased expression levels of phosphoenolpyruvate carboxykinase (PEPCK) and glucose transporter 2 (GLUT2), which are an enzyme in gluconeogenesis and a transporter of glucose, respectively (Lamia et al., 2008). Moreover, *Atrogin1*, which is a muscle-specific gene that regulates muscle atrophy, is directly controlled by clock genes (Andrews et al., 2010; Zhang et al., 2012). Furthermore, the E-box controls the expression rhythm of monoamine oxidase (MAO), which is an enzyme for the degradation of monoamine (Albrecht, 2017). Taken together, maintaining accurate expression rhythms of clock genes is important for maintaining physiological functions (Figure 1.1).

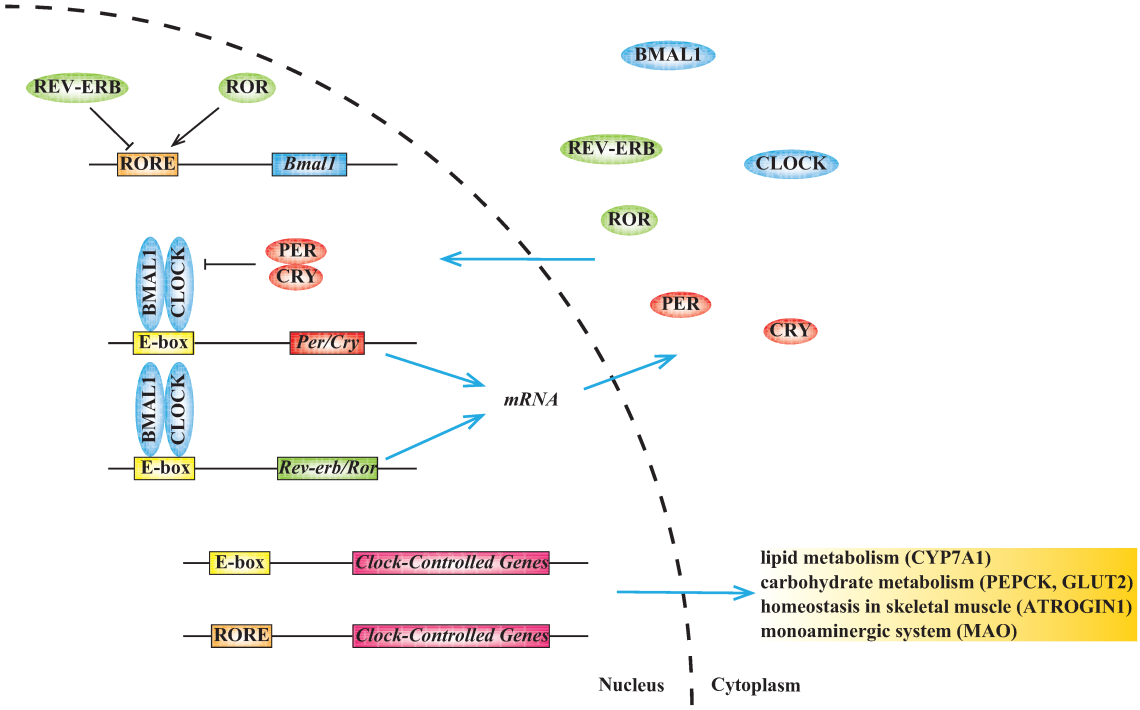

Figure 1.1 Schematic of negative transcriptional-translational feedback loops of clock genes

Transcription of *Per* and *Cry* are activated by heterodimers of CLOCK and BMAL1 in the nucleus, and *Per* and *Cry* mRNA are translated in the cytoplasm. Subsequently, the translated proteins reduce the transcription of their own mRNA by binding to heterodimers of CLOCK and BMAL1. As a result, this loop produces an approximately 24-hour cycle. Clock genes regulate the activity of specific promoter domains, such as the E-box and RORE, and circadian fluctuation, which lead to the regulation of the expression levels of clock-controlled genes. Representative genes controlled by clock genes are shown (Bass & Takahashi, 2010; Albrecht, 2017).

Mammals, including humans, have a central clock and peripheral clocks (Hastings, 1997; Weaver, 1998; Buijs et al., 2003). The central clock is located in the suprachiasmatic nucleus (SCN) of the hypothalamus, and the peripheral clocks are located in brain regions other than the SCN as well as in almost all peripheral organs. The central clock is entrained by the environmental LD signal through the retinal-hypothalamic tract, and the central clock orchestrates the peripheral clocks using neural signals, hormonal signals, locomotor activity, and other pathways (Nelson & Zucker, 1981; Albrecht, 2012). Accordingly, SCN-lesioned mice showed arrhythmic behavior, and their peripheral clocks were reduced in amplitude and rhythmicity (Mouret et al., 1978; Szafarczyk et al., 1981; Tahara et al., 2012). Whereas the central clock is entrained only by light, the peripheral clocks are not only synchronized with the central clock but are also reset by other types of stimulation, including food intake, exercise, and stress (Hara et al., 2001; Sasaki et al., 2016; Tahara et al., 2015) (Figure 1.2).

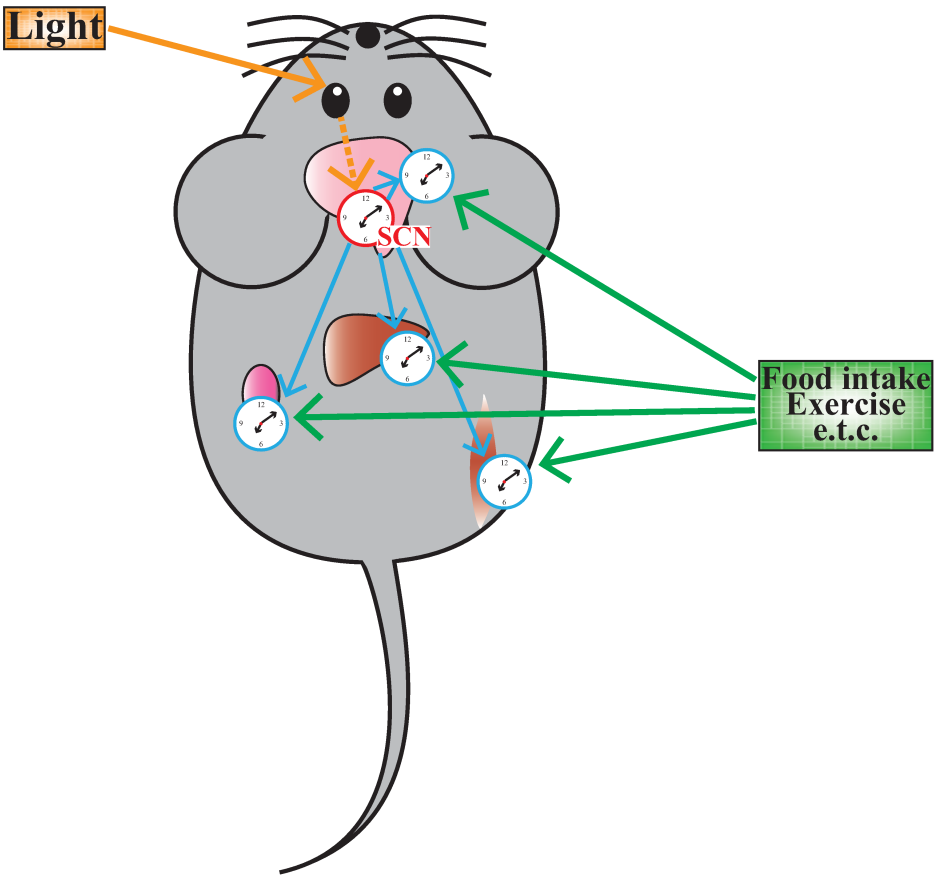

Figure 1.2 Association among light, other stimulations, the central clock, and peripheral clocks

The central clock (SCN; red clock) is entrained by the environmental LD signal through the retinal-hypothalamic tract (orange arrow and orange dashed arrow). The central clock orchestrates the peripheral clocks (blue clocks) by neural signals, hormonal signals, locomotor activity, and other pathways (blue arrows). The peripheral clocks are synchronized also with other stimulations, including food intake and exercise (green arrows).

Some reports showed that among the various types of stimulations, food intake is the strongest entrainment factor next to light (Garaulet & Madrid, 2010; Shibata et al., 2010; Delezie & Challet, 2011; Mistlberger, 2011). Especially, the timing of food intake and the composition of the consumed food are important synchronizers of peripheral clocks (Tahara & Shibata, 2016). Therefore, we would determine the optimal meal timing for maintaining and improving health, by clarifying the association among the circadian clock system, food intake, and metabolic system (Tahara & Shibata, 2013). Based on these previous studies, research on the association between the circadian clock system and food intake has been named chrono-nutrition (Tahara & Shibata, 2013). Research on chrono-nutrition has recently been increasing. A previous study in mice showed that l-ornithine, which is a type of non-protein amino acid, had an effect on the time-dependent phase shift of peripheral clocks *in vivo* (Fukuda et al., 2016). Another study showed that blood glucose levels in the glucose tolerance test depended on the time of day (Mi et al., 2017). Furthermore, a recent study in humans indicated that late meals delayed plasma glucose rhythm and clock gene expression rhythm in adipose tissue (Wehrens et al., 2017). In addition, blood glucose levels were increased after a late evening meal and subsequent breakfast. In the same study, the average blood glucose levels during a 24-hour period were also increased by a late meal (Sato et al., 2011). The Overview of Dietary Reference Intakes for Japanese (2015) has a chapter on the importance of breakfast and the timing of meals for the first time. This means that the study on meal patterns based on circadian rhythm has started to be recognized to play an important role in human health.

In this thesis, I aimed to analyze the association among circadian feeding patterns, obesity, and depressive-like behavior in mice based on the above previous research. Previous

studies indicated that high-fat diet (HFD)-induced obese mice show circadian arrhythmic locomotor activity and feeding rhythm (Kohsaka et al., 2007; Froy, 2012). Moreover, other previous studies suggested that depression is associated with phase shifts and decreases in melatonin rhythm, and disruptions of endogenous biological rhythms (Lewy, 2010; Nechita et al., 2015). Accordingly, I presumed that obesity and depression might closely interact with disturbance of the circadian clock system. Previous studies showed that circadian meal patterns affect the circadian clock system, particularly peripheral clocks; however, few studies have analyzed the association among circadian meal patterns, obesity, and depression. Therefore, I investigated the effects of circadian feeding patterns on obesity and depressive-like behavior in mice (Figure 1.3).

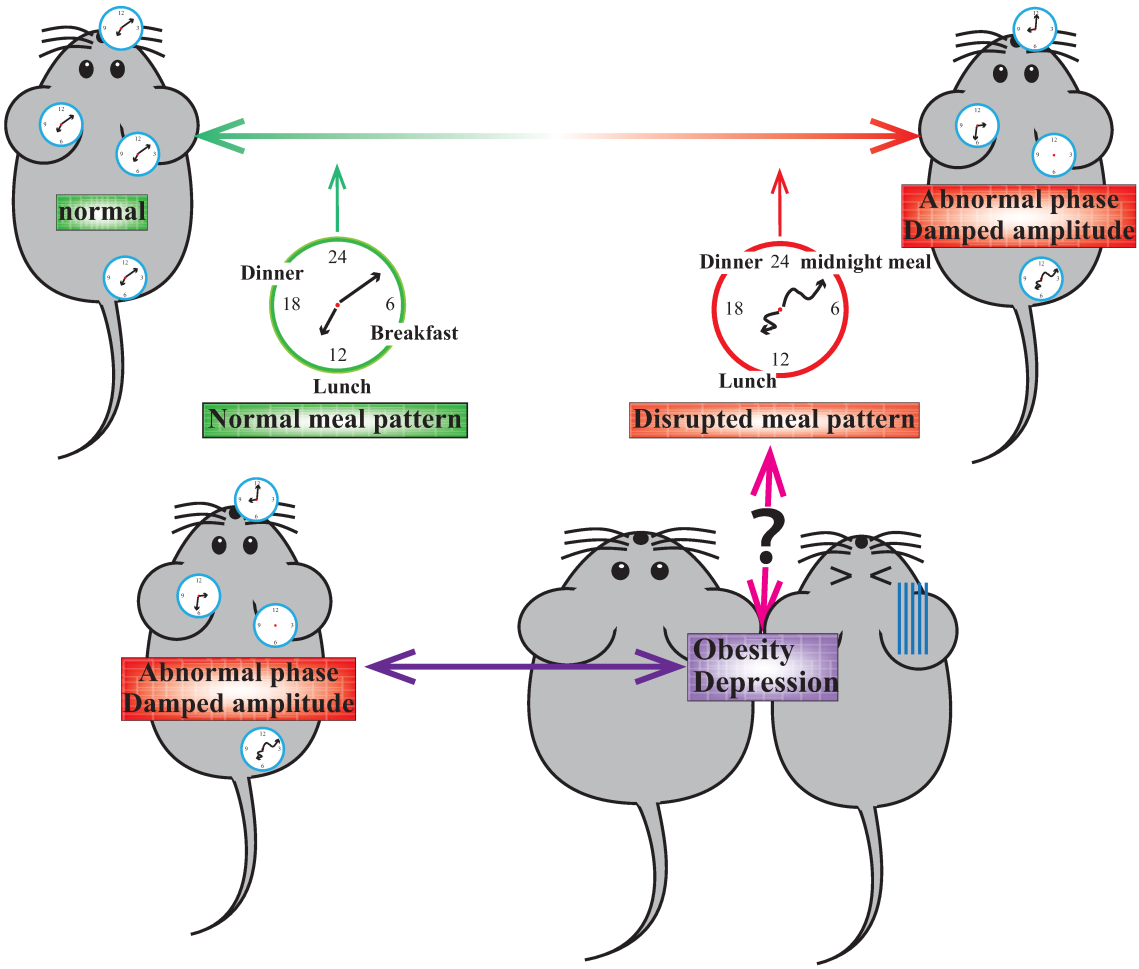

Figure 1.3 Working hypotheses of my thesis

An appropriate circadian meal pattern would maintain a precise circadian clock system (green arrow). On the contrary, a disrupted circadian meal pattern may decrease the amplitude and/or shift phase of peripheral clocks (red arrow) (Wehrens et al., 2017). Moreover, obese mice showed arrhythmic circadian locomotor activity and feeding rhythm (Froy, 2012), and depression was found to be associated with disruptions of endogenous biological rhythm (Lewy, 2010; Nechita et al., 2015) (purple two-way arrow). However, few studies have analyzed the association among circadian meal patterns, obesity, and depression (pink two-way arrow and question mark). Therefore, I investigated the effects of circadian feeding patterns on obesity and depressive-like behavior in mice.

Chapter 2. Effects of the timing and duration of HFD administration on the obesity of mice

2.1 Introduction

Adult obesity is now observed in about 13% of the general population (World Health Organization, 2016), and one of the major factors of obesity is excessive calorie intake. Excessive calorie intake has the potential to cause hyperleptinemia, insulin resistance, glucose intolerance, and increased adiposity. A previous study suggested that energy homeostasis interacts with the circadian clock system at the molecular, behavioral, and physiological levels (Bass & Takahashi, 2010). Free feeding (FF) with a HFD affected energy metabolism, decreased the amplitude and/or shifted the phase of clock gene expression rhythms in the liver, and increased calorie intake during the resting phase (the light period), compared with FF with a normal-fat diet (ND) (Kohsaka et al., 2007; Froy, 2012). Moreover, body weights of mice were more increased by restricted feeding (RF) with a HFD during the resting phase than that under RF with a HFD during the active phase (the dark period) (Arble et al., 2009; Salgado-Delgado et al., 2010). With regard to mice, the light and dark periods are called the resting and active phases, respectively, because mice are nocturnal animals. Under 4-hour RF with a HFD during the resting phase or 8-hour RF during the active phase, RF suppressed the HFD-induced decrease in amplitude and phase shift of clock gene expression rhythms in the liver, as well as body weight gain (Sherman et al., 2012; Hatori et al., 2012). Taken together, these results indicate that RF is an important feeding treatment for preventing HFD-induced obesity and disruption of the circadian clock system. However, there have been no studies on the effects of

differences in RF with a HFD between during the resting and active phases, or differences in RF duration on obesity and the circadian clock system.

To investigate the effects of these differences, I fed mice with a HFD during the resting phase and a ND during the active phase ([HFD-ND]), or a ND during the resting phase and a HFD during the active phase ([ND-HFD]). Mice had access to a ND or a HFD for a given duration (2, 4, 8, or 12 hours per phase). I have 2 hypotheses in this chapter. First, I hypothesized that body weight gain might depend on feeding patterns. Accordingly, I expected that body weights in the [HFD-ND] group might increase more rapidly than those in the [ND-HFD] group. Second, I hypothesized that body weight gain might also depend on RF duration. Therefore, I anticipated that body weights in the 2-hour RF groups, in which each RF duration was 2 hours, might be less increased than those in the other groups. Furthermore, conversely, I anticipated that body weights in the 8-8[HFD-ND] group, in which mice were subjected to 8-hour RF with a HFD during the resting phase and 8-hour RF with a ND during the active phase, would be greater than those in the other groups. Therefore, I analyzed the combination effect of RF duration and feeding pattern on body weight and visceral fat.

The other aims in this chapter were to investigate whether the timing and duration of intake of a HFD affects energy homeostasis and clock gene expression rhythms in the liver. A recent study has demonstrated that FF with a HFD for 1 week advanced the phase of the liver clock by 5 hours (Pendergast et al., 2013). Moreover, obesity was found to be closely associated with disturbance of the circadian clock system (Froy, 2012). Therefore, in this cahpter, I also analyzed the phases of peripheral clocks under RF treatment fed two meals a day. *In vivo* imaging system (IVIS) and PERIOD2::LUCIFERASE (PER2::LUC) knock-in mice enable us

to measure the circadian rhythms of peripheral organs noninvasively in individual mice *in vivo* (Yoo et al., 2003; Tahara et al., 2012).

This chapter is based on a manuscript by myself and others that was published by Taylor & Francis in *Chronobiology International* on Oct 2014, which is available online at http://www.tandfonline.com/10.3109/07420528.2014.931413. Consent from all authors has been obtained.

2.2 Materials and methods

2.2.1 Animals

Two types of mice were used, as follows: wild-type ICR mice and heterozygous PER2::LUC knock-in mice (a mixed background of C57/BL6J and ICR). Eight-week-old male ICR mice and male heterozygous PER2::LUC knock-in mice were housed in an animal room maintained at 22 °C ± 2 °C and 60% ± 5% humidity under a 12-hour light/12-hour dark cycle (lights on from 8:00 to 20:00). Zeitgeber time 0 (ZT 0) was defined as the lights-on time and ZT 12 was defined as the lights-off time. Heterozygous PER2::LUC knock-in mice were bred in our laboratory and housed in the animal room as previously described (Tahara et al., 2012). The mice had free access to a ND (EF; Oriental Yeast Co. Ltd., Tokyo, Japan) and water all day before the experiments started. The procedures conformed to the "Fundamental Guidelines for Proper Conduct of Animal Experiments and Related Activities in Academic Research Institutions" (published by the Ministry of Education, Culture, Sports, Science and Technology, Japan) and were approved by the Committee for Animal Experimentation at Waseda University (Permission no. 2013-A070).

2.2.2 Diets

Mice were fed with a ND and/or a HFD. Calories from fat were 10% in the ND and 44.9% in the HFD (D12451M; RESEARCH DIETS Inc., Tokyo, Japan).

2.2.3 Experimental procedures

Mice were fed with a ND and/or a HFD twice a day, during the active and resting

phases for 4 weeks. RF duration was controlled (2, 4, 8, or 12 hours per phase). Calorie intake was estimated by food intake, which was measured twice a week by monitoring the weight of the eaten food.

2.2.4 Effects of 4-hour RF with a ND or a HFD during the active and resting phases on obesity (Experiment 2.1)

Six groups were prepared, as follows: FF with a ND or a HFD (FF[ND] or FF[HFD]), 4-hour RF with a ND or a HFD during the resting and active phases (4-4[ND-ND] or 4-4[HFD-HFD]), 4-hour RF with a ND during the resting phase and a HFD during the active phase or vice versa (4-4[ND-HFD] or 4-4[HFD-ND]) (Figure 2.1A). Each feeding treatment group had one or two units. In each unit, four mice were housed in the home cage. Calorie intake was measured per group and expressed as kcal/mouse/day.

2.2.5 Effects of 2-, 4-, or 8-hour RF with a ND or a HFD during the active and resting phases on obesity (Experiment 2.2)

Six groups of mice were prepared, as follows: 2-hour RF with a ND during the resting phase and a HFD during the active phase or vice versa (2-2[ND-HFD] or 2-2[HFD-ND]), 4-hour RF with a ND during the resting phase and a HFD during the active phase or vice versa (4-4[ND-HFD] or 4-4[HFD-ND]), and 8-hour RF with a ND during the resting phase and a HFD during the active phase or vice versa (8-8[ND-HFD] or 8-8[HFD-ND]) (Figure 2.1B). Each feeding treatment group had two units. In each unit, three or four mice were housed in the home cage. Calorie intake was measured per group and expressed as kcal/mouse/day.

2.2.6 Effects of 2- or 4-hour RF with a ND or a HFD during the active and resting phases on obesity and postprandial blood glucose levels (Experiment 2.3)

Four groups were prepared as described for the 2- and 4-hour RF groups in experiment 2.2. Each mouse was housed individually in the home cage. The amount of food intake per mouse was monitored. After 4 weeks under each feeding treatment, postprandial blood glucose levels were measured (Figure 2.1C). Each group comprised four or five mice, and each mouse was housed in an individual cage. Calorie intake was measured per mouse and expressed as kcal/mouse/day.

2.2.7 Effects of 2-hour RF with a HFD during the resting phase and 2-, 6-, or 12-hour RF with a ND during the active phase on obesity (Experiment 2.4)

Three groups of mice were prepared, as follows: 2-hour RF with a HFD during the resting phase and a ND during the active phase (2-2[HFD-ND]), 2-hour RF with a HFD during the resting phase and 6-hour RF with a ND during the active phase (2-6[HFD-ND]), and 2-hour RF with a HFD during the resting phase and 12-hour RF with a ND during the active phase (2-12[HFD-ND]) (Figure 2.1D). Each feeding treatment group had one or two units. In each unit, four mice were housed in the home cage. Calorie intake was measured per group and expressed as kcal/mouse/day.

2.2.8 Effects of each feeding treatment on phase of the liver clock (Experiment 2.5)

Nine groups of mice were chosen from experiments 2.1, 2.2, and 2.4, as follows:

FF[ND], FF[HFD], 4-4[ND-ND], 4-4[HFD-HFD], 4-4[ND-HFD], 4-4[HFD-ND], 2-2[HFD-ND], 8-8[HFD-ND], and 2-12[HFD-ND]. Heterozygous PER2::LUC knock-in mice were maintained under each feeding treatment for 3 or 4 weeks, and then the peak phase of PER2 rhythm in the liver was measured by *in vivo* monitoring of bioluminescence.

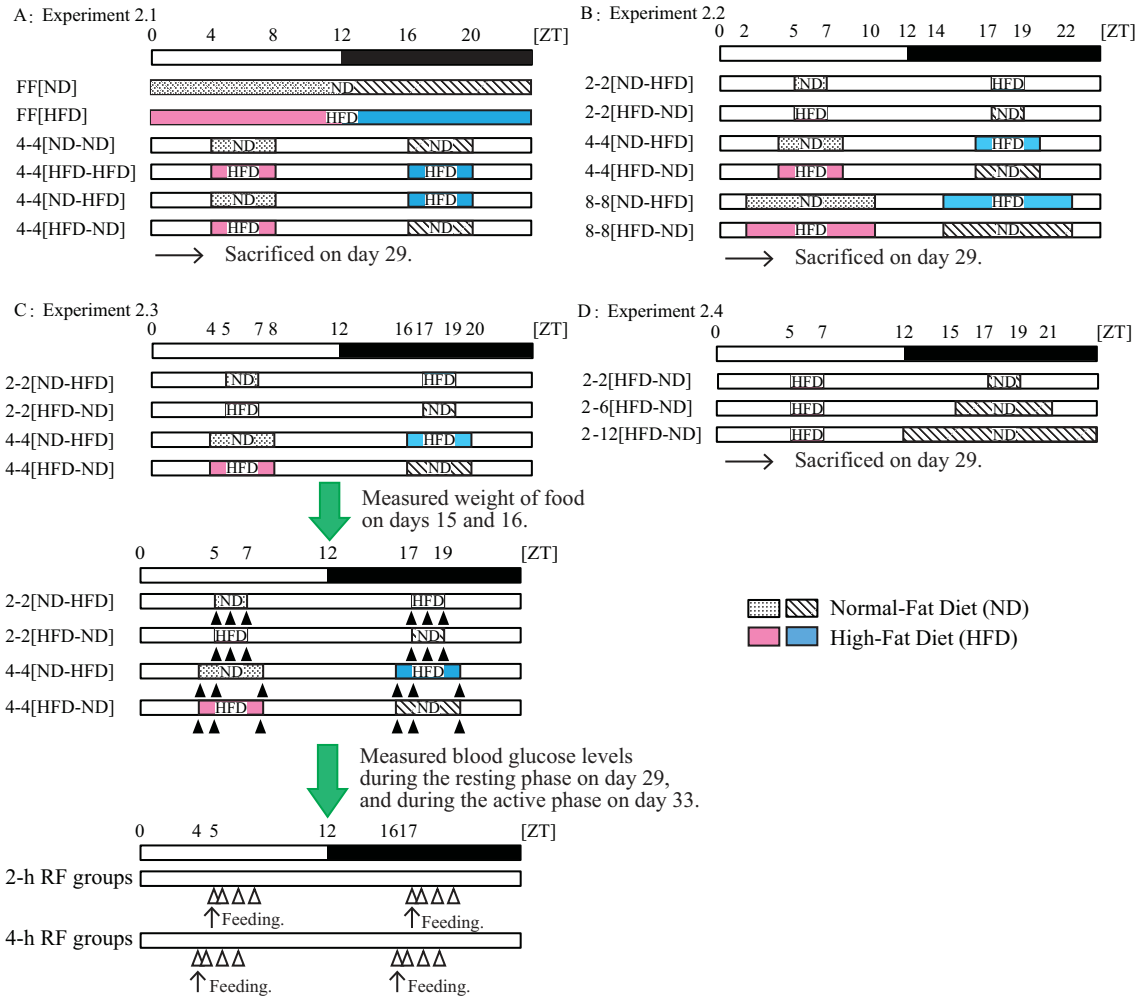

Figure 2.1 Experimental feeding treatments

ICR mice were fed with a ND and/or a HFD for 4 weeks according to the feeding treatments shown. Open and closed bars indicate the resting and active phases, respectively. (A) Experiment 2.1: FF groups and 4-hour RF groups. Mice were housed with mice in the same groups and sacrificed on day 29. (B) Experiment 2.2: 2-, 4-, and 8-hour RF groups. Mice were housed with mice in the same group and sacrificed on day 29. (C) Experiment 2.3: 2- or 4-hour RF groups. Mice were housed individually. Food intake was measured during the initial hour of feeding on days 15 and 16. Postprandial blood glucose levels were measured during the resting phase on day 29. Four days later, on day 33, postprandial blood glucose levels were measured

during the active phase. Black triangles represent the time points when the weight of the food was measured, and white triangles represent the time points when blood was collected for measuring postprandial blood glucose levels. (D) Experiment 2.4: 2-hour RF with a HFD during the resting phase and 2-, 6-, or 12-hour RF with a ND during the active phase. Mice were housed with mice in the same group and sacrificed on day 29. These figures have been modified and reprinted from Figure 1 of Haraguchi et al. (2014).

2.2.9 Time course measurements of postprandial blood glucose levels

In experiment 2.3, postprandial blood glucose levels were measured in each group. At the start of the feeding period of each group at ZT 4 (4-hour RF groups) or ZT 5 (2-hour RF groups), mice were fed with a ND (0.2 g) or a HFD (1.0 g). In the preliminary experiments, to determine the appropriate amount of food that can be eaten within 30 minutes by the mice, the amount of food intake during the initial 30 minutes in the active and resting phases were measured. Postprandial blood glucose levels were measured before (0 minutes) and 30, 75, and 150 minutes after feeding. After four days, the same protocol was performed at each group's feeding time at ZT 16 (4-hour RF groups) or ZT 17 (2-hour RF groups). The area under the blood glucose concentration time curve (AUC) was estimated for all groups. One drop of blood was collected from the tail vein, and the glucose concentrations were measured using a Glucose PILOT kit (Aventir Biotech, CA, USA).

2.2.10 *In vivo* monitoring protocol and data analysis

In vivo monitoring system was performed as previously described (Tahara et al., 2012). In brief, *in vivo* monitoring system was performed using a IVIS kinetics system (Caliper Life Sciences, MA, USA). Mice were anesthetized in the IVIS kinetics system with isoflurane (Mylan Inc., Tokyo, Japan) and concentrated oxygen (SO-005B; Sanyo Electronic Industries Co. Ltd., Okayama, Japan) using a gas anesthesia system (XGI-8; Caliper Life Sciences). After mice were anesthestized, they were injected subcutaneously on the back and near the neck with D-luciferin potassium salt (Promega, WI, USA), at a dose of 15 mg/kg of body weight (30 mg/10 mL, 0.05 mL/10 g body weight). Images were taken at 10 minutes after injection in the

ventral-up position for pictures of the liver. Each image was taken using a 1-minute exposure time. For each time point, the bioluminescence images were merged with the grey-scale image. Images were obtained six times per day (ZT 11, 15, 19, 23, 3, and 7). Mice were returned to their home cages after each imaging procedure and recovered quickly from isoflurane anesthesia. The duration under isoflurane anesthesia was approximately 20 minutes per session. A previous study confirmed that anesthesia and bioluminescence analysis every 4 hours did not affect luciferase activity in the peripheral tissues or the behavior of the mice (Tahara et al., 2012).

Bioluminescence emitted from the liver was estimated using Living Image 3.2 software (Caliper Life Sciences). The region of interest (ROI) was set to the same shape and size for all experiments. The average photon/minute values of the data from the six time points for each day was designated as 100%, and the bioluminescence rhythm for the entire day was expressed as a percentage of each set of six time points for the liver. The peak phase and amplitude of the normalized percentage data were estimated using the single cosinor procedure program (Acro.exe, version 3.5) (Refinetti et al., 2007).

2.2.11 Measurement of visceral fat weight

In experiments 2.1, 2.2, and 2.4, mice were maintained under specific feeding treatments for 4 weeks before sacrifice. All mice were fasted from ZT 19 and then sacrificed at ZT 2. Visceral fat was dissected from each mouse and the weights of visceral adipose tissue were measured.

2.2.12 Statistical analysis

Data are expressed as the mean ± standard error of the mean (SEM). For statistical analysis, a one-way or two-way analysis of variance (ANOVA) was applied using StatView software, and post-hoc analysis was conducted using the Tukey-Kramer test (SAS Institute, NC, USA). A *p*-value of less than 0.05 was considered to indicate a statistically significant difference between 2 groups.

2.3 Results

2.3.1 Effects of 4-hour RF with a ND or a HFD during the active and resting phases on obesity (Experiment 2.1)

In experiment 2.1, the effects of 4-hour RF with a ND or a HFD on body weight gain and visceral fat were analyzed. Each feeding treatment is explained in Experimental procedures (Figures 2.1A and 2.2A). The total calorie intake in the FF[HFD] group was more than that in the FF[ND] group (Figure 2.2B). Although mice were fed with a HFD in the 4-4[HFD-HFD], 4-4[ND-HFD], and 4-4[HFD-ND] groups, the total calorie intake in the three groups was similar to that in the FF[ND] group (Figure 2.2B). In the RF groups, calorie intake was measured during the active phase (ZT 16-20) and resting phase (ZT 4-8). Mice in the 4-4[HFD-ND] group had a higher calorie intake during the resting phase than during the active phase (Figure 2.2B), whereas mice in the other RF groups had a higher calorie intake during the active phase (Figure 2.2B). Body weights in the FF[HFD] group were higher than those in the FF[ND] group. There were significant differences in body weight increases among the six groups (one-way ANOVA; $F(5,38) = 6.0$, $p < 0.001$) (Figure 2.2C). The 4-4[ND-ND], 4-4[ND-HFD], and 4-4[HFD-ND] groups showed significantly less body weight gain than the FF[HFD] group, but the 4-4[HFD-HFD] group showed no significantly less body weight gain than the FF[HFD] group (Figure 2.2C). When the ratio of body weight increase to total calorie intake was estimated (Figure 2.2D), the change was similar to the change in body weight increase. A ratio of the amount of visceral fat to body weight in the FF[ND] group was similar to that in the 4-4[ND-ND] and 4-4[ND-HFD] groups, but the ratios in the FF[HFD] and 4-4[HFD-HFD] groups were higher than those in the other groups. Furthermore, there were

significant differences among the six groups. There was no significant difference between the 4-4[ND-HFD] and 4-4[HFD-ND] groups (Figure 2.2E). These results suggest that the 4-hour RF with a ND during the resting phase suppresses the increase in body weights and the accumulation of visceral fat by the 4-hour RF with a HFD during the active and resting phases.

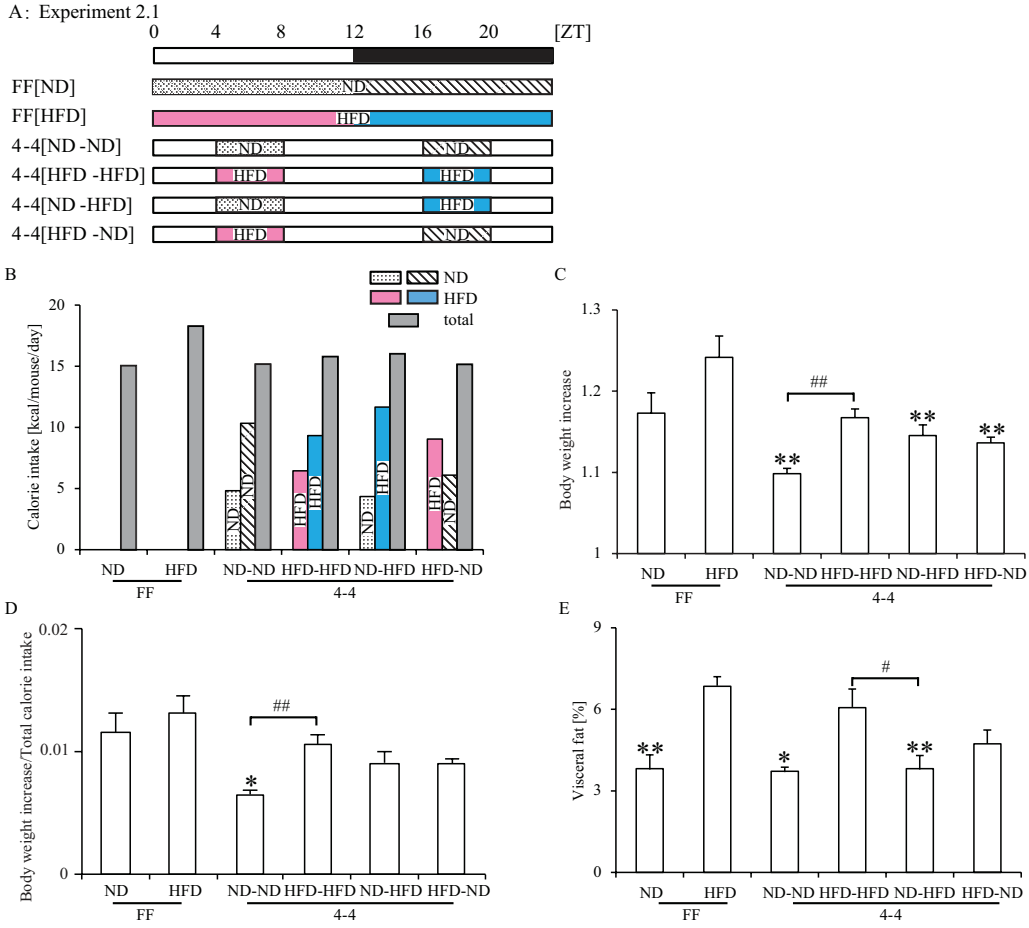

Figure 2.2 Effects of FF or 4-hour RF on calorie intake, body weight, and visceral fat (Experiment 2.1)

(A) Feeding treatments. Open and closed bars indicate the resting and active phases, respectively. (B) Average calorie intake per group for 4 weeks. Each feeding treatment group had one or two units. In each unit, four mice were housed in the same cage. For all groups, the gray columns on the right indicate total calorie intake, the left columns indicate calorie intake during the resting phase, and the center columns indicate calorie intake during the active phase. (C) Relative body weight increases after 4 weeks under each feeding treatment. Body weights at the start of feeding treatments were set to 1. (D) Ratios of body weight increase to calorie intake. Vertical-axis: (body weight increase – 1)/average total calorie intake per group for 4 weeks. (E)

Visceral fat percentages. Vertical-axis: (adipose tissue weight/body weight) × 100 (%). (FF[ND], n = 8; FF[HFD], n = 8; 4-4[ND-ND], n = 4; 4-4[HFD-HFD], n = 8; 4-4[ND-HFD], n = 8; 4-4[HFD-ND], n = 8). * $p < 0.05$, ** $p < 0.01$ vs. FF[HFD] (Tukey-Kramer test). # $p < 0.05$, ## $p < 0.01$ for 4-4[HFD-HFD] vs. the other 4-hour RF groups (Tukey-Kramer test). These figures have been modified and reprinted from Figure 2 of Haraguchi et al. (2014).

2.3.2 Effects of 2-, 4-, or 8-hour RF with a ND or a HFD during the active and resting phases on obesity (Experiment 2.2)

In experiment 2.2, the effects of RF duration on body weight gain and visceral fat were measured. Each feeding treatment is explained in Experimental procedures (Figures 2.1B and 2.3A). The total calorie intake was positively associated with RF duration (Figure 2.3B). Two-way ANOVA demonstrated the interaction of feeding pattern × RF duration with only visceral fat ($F(2,41) = 3.27$, $p = 0.048$). In the 2- and 4-hour RF groups, body weight increase, ratio of body weight increase to total calorie intake, and ratio of the amount of visceral fat to body weight in the ND-HFD groups were similar to those in the HFD-ND group (Figures 2.3C-2.3E). On the contrary, body weight increase, ratio of body weight increase to total calorie intake, and ratio of the amount of visceral fat to body weight in the 8-8[HFD-ND] group were higher than those in the 8-8[ND-HFD] group (Figures 2.3C-2.3E). Body weight increase and visceral fat in the 2-hour RF groups and the 8-8[HFD-ND] group were significantly heavier than their counterparts of the 4-hour RF groups (Figures 2.3C-2.3E). Taken together, these results indicate that a short RF duration, such as in the 2-hour RF groups, enhances the effect of a HFD on body weight increase and the accumulation of visceral fat, contrary to my hypothesis.

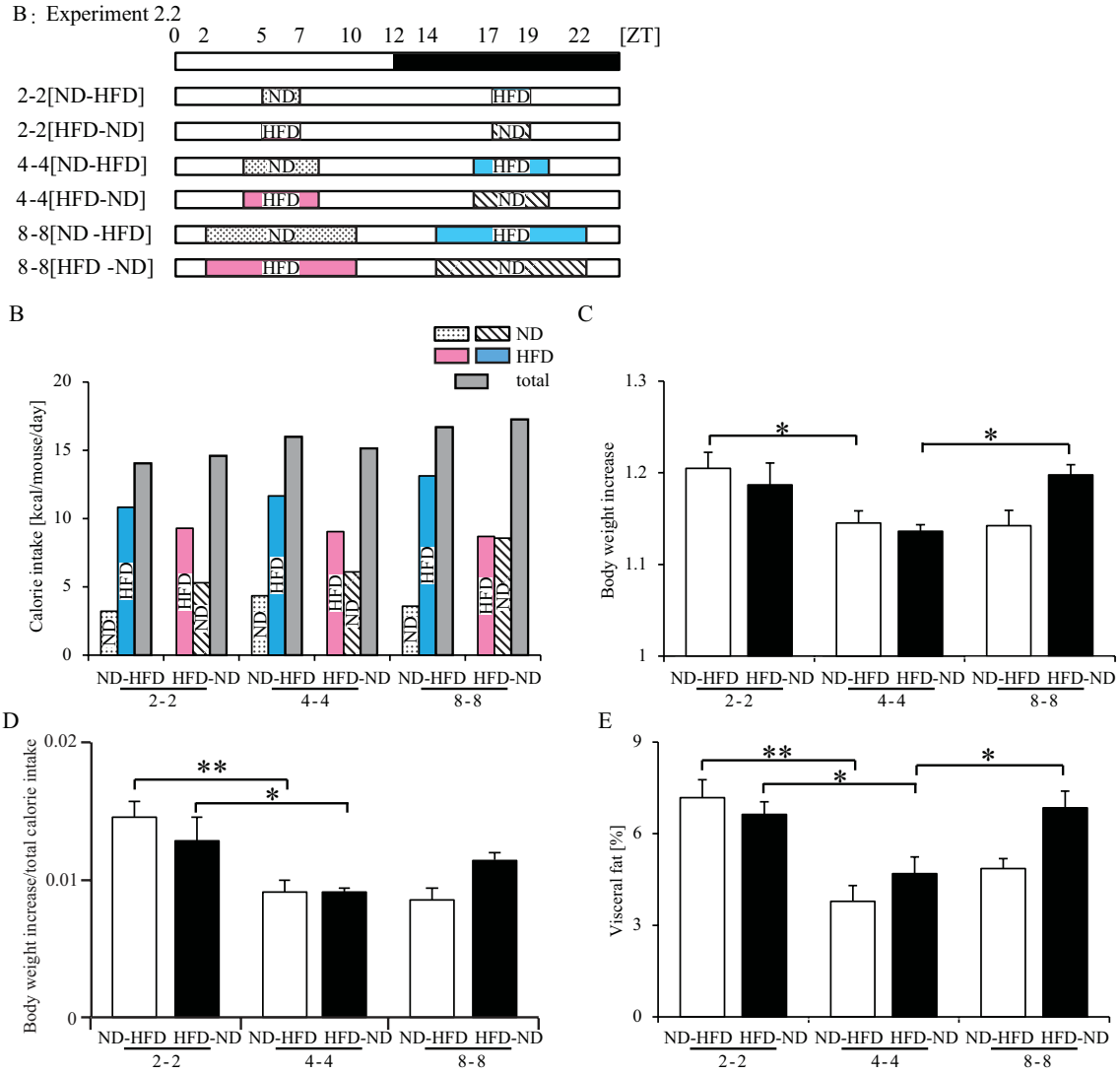

Figure 2.3 Effects of 2-, 4-, or 8-hour RF on calorie intake, body weight, and visceral fat (Experiment 2.2)

(A) Feeding treatments. Open and closed bars indicate the resting and active phases, respectively. (B) Calorie intake per group for 4 weeks. Each feeding treatment group had two units. In each unit, three or four mice were housed in the same cage. The left columns indicate calorie intake during the resting phase, the center columns indicate calorie intake during the active phase, and the gray columns on the right indicate total calorie intake. (C) Relative body weight increases after 4 weeks. For each group, body weights at the start of the feeding

treatments were set to 1. (D) Ratios of body weight increase to total calorie intake. Vertical-axis: (body weight increase – 1)/average total calorie intake per group over 4 weeks. (E) Visceral fat percentages. Vertical-axis: (adipose tissue weight/body weight) × 100 (%). Data are presented as the mean ± SEM (2-2[ND-HFD], n = 8; 2-2[HFD-ND], n = 8; 4-4[ND-HFD], n = 8; 4-4[HFD-ND], n = 8; 8-8[ND-HFD], n = 8; 8-8[HFD-ND], n = 7). * $p < 0.05$, ** $p < 0.01$ (Tukey-Kramer test). These figures have been modified and reprinted from Figure 3 of Haraguchi et al. (2014).

2.3.3 Effects of 2- or 4-hour RF with a ND or a HFD during the active and resting phases on obesity and postprandial blood glucose levels (Experiment 2.3)

In experiment 2.2, I observed that a 2-hour RF treatment did not appear to suppress HFD-induced obesity. Therefore, in experiment 2.3, to clarify the reason of these results, I compared body weight increase, eating speed, and postprandial blood glucose level in the 2- and 4-hour RF groups. Each feeding treatment is described in detail in Experimental procedures (Figures 2.1C and 2.4A). I measured the amount of food intake in individual mice. There were no significant differences in the total calorie intake when the data were analyzed by one-way ANOVA ($F(1,15) = 0.09$, $p = 0.76$) (Figure 2.4B). However, when calorie intake was measured during the initial hour of each RF, there were significant differences in total calorie intake (one-way ANOVA, $F(1,15) = 29.7$, $p = 0.001$) (Figure 2.4C). Although there were no significant differences in body weight increase among the four groups, a significant difference in the ratio of body weight increase to total calorie intake was found between the 2-2[ND-HFD] and 4-4[ND-HFD] groups (Figures 2.4D and 2.4E). I measured the postprandial blood glucose levels in the four groups. During the resting phase, mice were fed with a ND (Figure 2.4F) or a HFD (Figure 2.4G), and their blood glucose levels were measured before (0 minutes) and 30, 75, and 150 minutes after feeding. In the 2-2[HFD-ND] group, the postprandial blood glucose levels were higher than those in the 4-4[HFD-ND] group. The AUC in the 2-2[HFD-ND] group was significantly higher than that in the 4-4[HFD-ND] group (Figure 2.4G). During the active phase, mice were fed with a ND (Figure 2.4H) or a HFD (Figure 2.4I). Postprandial blood glucose levels in the 2-2[HFD-ND] group were higher than those in the 4-4[HFD-ND] group (Figure 2.4H). These results suggest that short-term calorie intake impairs glucose tolerance,

leading to obesity.

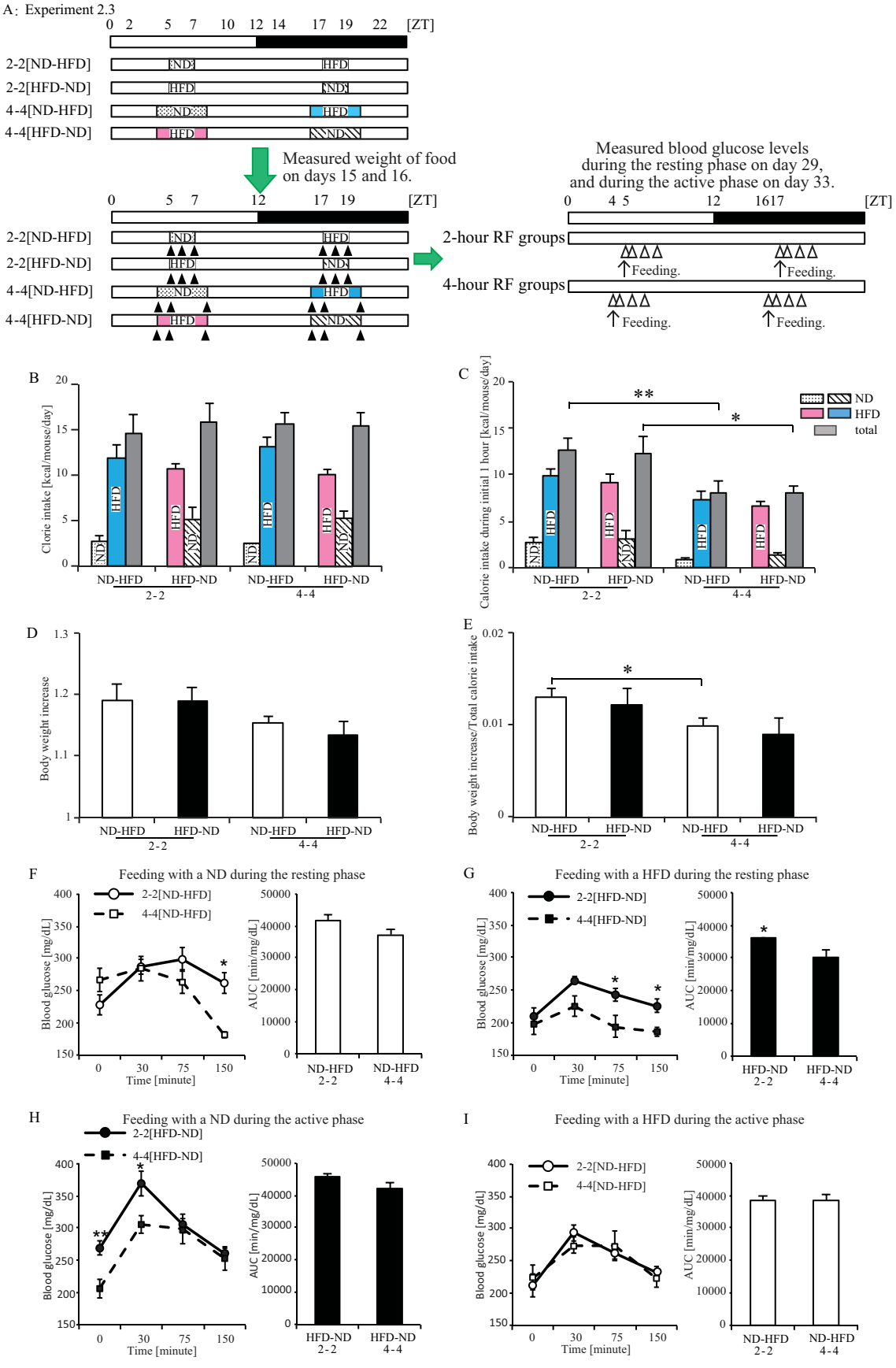
A: Experiment 2.3
0 2 5 7 10 12 14 17 19 22 [ZT]
2-2[ND-HFD]
2-2[HFD-ND]
4-4[ND-HFD]
4-4[HFD-ND]
ND
HFD
Measured weight of food on days 15 and 16.
0 5 7 12 17 19 [ZT]
Measured blood glucose levels during the resting phase on day 29, and during the active phase on day 33.
0 4 5 12 1617 [ZT]
2-hour RF groups
4-hour RF groups
Feeding.
B
Clorie intake [kcal/mouse/day]
ND-HFD
HFD-ND
2-2
4-4
C
Calorie intake during initial 1 hour [kcal/mouse/day]
ND
HFD
total
D
Body weight increase
E
Body weight increase/Total calorie intake
F
Feeding with a ND during the resting phase
2-2[ND-HFD]
4-4[ND-HFD]
Blood glucose [mg/dL]
AUC [min/mg/dL]
Time [minute]
G
Feeding with a HFD during the resting phase
2-2[HFD-ND]
4-4[HFD-ND]
H
Feeding with a ND during the active phase
I
Feeding with a HFD during the active phase

Figure 2.4 Effects of 2- or 4-hour RF on body weights, eating speeds, and postprandial blood glucose levels (Experiment 2.3)

(A) Feeding treatments. Open and closed bars indicate the resting and active phases, respectively. Food intake was measured during the initial hour of feeding on days 15 and 16. Postprandial blood glucose levels during the resting phase on day 29. Four days later, postprandial blood glucose levels were measured during the active phase on day 33. The black triangles represent the time points when the weight of the food was measured, and the white triangles represent the time points when blood was collected for measuring the postprandial blood glucose levels. (B) Calorie intake in each group throughout the experiment. The left columns indicate calorie intake during the resting phase, the center columns indicate calorie intake during the active phase, and the gray columns on the right indicate total calorie intake. (C) Calorie intake in each group during the first hour after feeding on days 15 and 16. (D) Relative body weight increases after 4 weeks. For each group, body weights at the start of the feeding treatments were set to 1. (E) Ratios of body weight increase to total calorie intake. Vertical-axis: (body weight increase – 1)/average total calorie intake for 4 weeks. (F and G) Time course of postprandial blood glucose levels in mice fed with 0.2 g of a ND (F) or 1.0 g of a HFD (G) during the resting phase on day 29 (starting at ZT 4 or 5), and the area under the blood glucose concentration time curve (AUC) values. (H and I) Time course of postprandial blood glucose levels in mice fed with 0.2 g of a ND (H) or 1.0 g of a HFD (I) during the active phase on day 33 (starting at ZT 16 or 17), and the AUC values. Data are presented as the mean ± SEM (2-2[ND-HFD], n = 5; 2-2[HFD-ND], n = 4; 4-4[ND-HFD], n = 5; 4-4[HFD-ND], n = 5). * $p < 0.05$, ** $p < 0.01$ (Student *t*-test). These figures have been modified and reprinted from

Figure 4 of Haraguchi et al. (2014).

2.3.4 Effects of 2-hour RF with a HFD during the resting phase and 2-, 6-, or 12-hour RF with a ND during the active phase on obesity (Experiment 2.4)

In experiment 2.2, the 8-8[HFD-ND] group had a higher calorie intake during the resting phase than during the active phase, and their body weight and visceral fat were higher than those in the 8-8[ND-HFD] group. Therefore, in experiment 2.4, to understand whether the ratio of calorie intake during the active phase to that during the resting phase is an important factor for obesity, I compared body weight increases and visceral fat volumes in the 2-2[HFD-ND], 2-6[HFD-ND], and 2-12[HFD-ND] groups. Each feeding treatment is described in detail in Experimental procedures (Figures 2.1D and 2.5A). The duration of RF with a ND was positively associated with calorie intake from a ND (Figure 2.5B). Although mice were fed with a HFD during the resting phase, the 2-6[HFD-ND] and 2-12[HFD-ND] groups had a higher calorie intake during the active phase than during the resting phase, whereas the 2-2[HFD-ND] group did not (Figure 2.5B). Body weight increases, ratios of body weight increase to total calorie intake, and ratios of the amount of visceral fat to body weight were more increased in the 2-2[HFD-ND] group than in the 2-6[HFD-ND] and 2-12[HFD-ND] groups (Figures 2.5C-2.5E). These results indicate that to maintain the calorie intake during the active phase higher than that during the resting phase would be an important factor in preventing obesity induced by RF with a HFD during the resting phase.

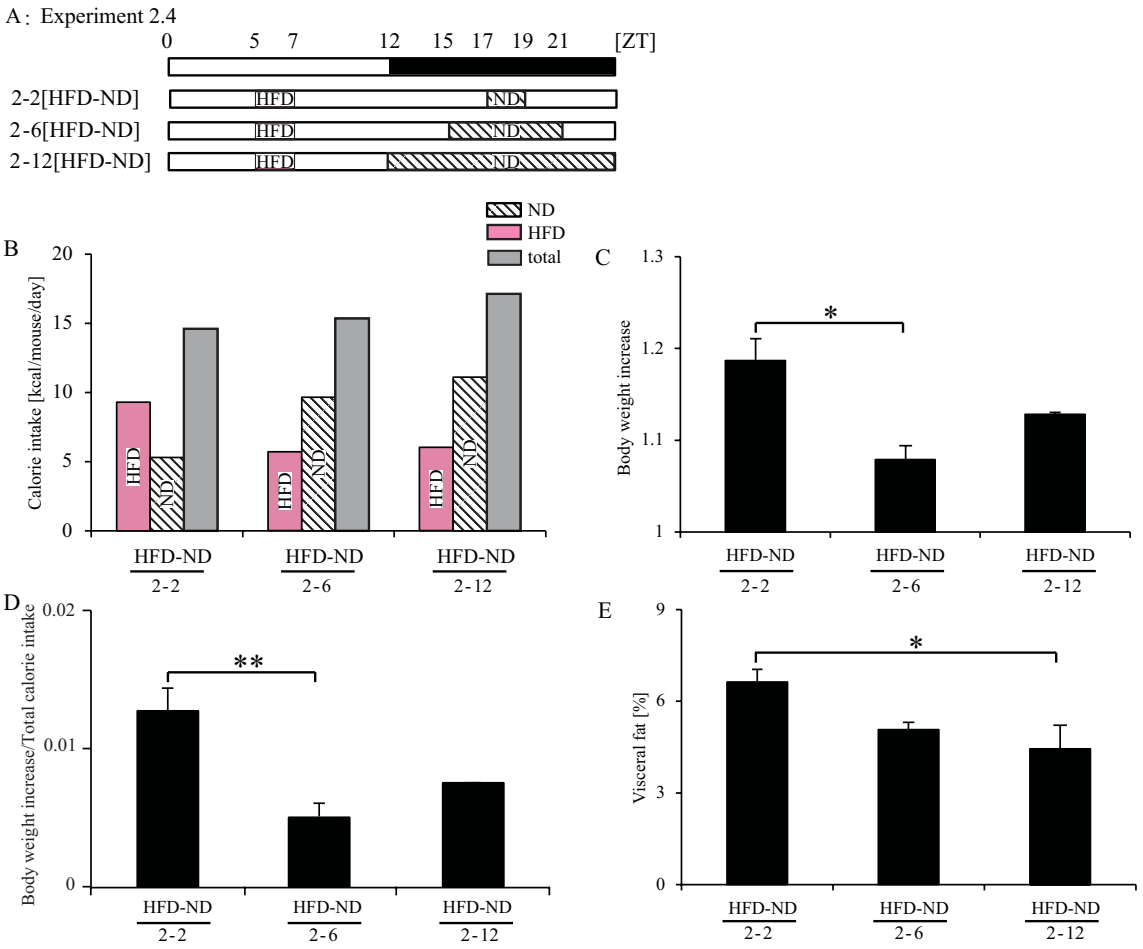

Figure 2.5 Effects of 2-hour RF with a HFD during the resting phase and 2-, 6-, or 12-hour RF with a ND during the active phase on calorie intake, body weight, and visceral fat (Experiment 2.4)

(A) Feeding treatments. Open and closed bars indicate the resting and active phases, respectively. (B) Calorie intake per group over 4 weeks. Each feeding treatment group had one or two units. In each unit, four mice were housed in the same cage. The left columns indicate calorie intake during the rest phase, the center columns indicate calorie intake during the active phase, and the right gray columns indicate total calorie intake. (C) Relative body weight increases after 4 weeks. For each group, body weights at the start of each feeding treatment were set to 1. (D) Ratios of body weight increase to total calorie intake. Vertical-axis: (body

weight increase – 1)/average total calorie intake over 4 weeks. (E) Visceral fat percentages. Vertical-axis: (adipose tissue weight/body weight) × 100 (%). Data are presented as the mean ± SEM (2-2[HFD-ND], n = 8; 2-6[HFD-ND], n = 4; 2-12[HFD-ND], n = 4). * $p < 0.05$, ** $p < 0.01$ (Tukey-Kramer test). These figures have been modified and reprinted from Figure 5 of Haraguchi et al. (2014).

2.3.5 Effects of each feeding treatment on the phase of the liver clock (Experiment 2.5)

Previous studies suggested that FF with a HFD decreased the amplitude and/or shifted the phase of clock gene expression rhythms in the liver (Kohsaka et al., 2007; Froy, 2012), and that a HFD induced obesity. In brief, one of the causes of HFD-induced obesity might be an alteration of peripheral clocks (decreased amplitude and/or phase shift). Therefore, in experiment 2.5, I analyzed the effects of different feeding treatments on the peripheral clock in the liver. A previous study indicated that the phase of the peripheral clock can be entrained not only by the timing and composition of food but also by the amount of calorie intake (Hirao et al., 2010). From experiment 2.1-2.4, in the HFD-ND groups, the amount of calorie intake from a HFD during the resting phase was more than that of a ND during the active phase. On the other hand, in the other groups, the amount of calorie intake during the active phase was more than that during the resting phase. I analyzed the phase of the liver clock using an *in vivo* monitoring system under RF with a HFD and/or a ND. Figure 2.6A shows an example of the daily rhythm of bioluminescence expressed as relative activity (%) in the 4-4[ND-ND], 4-4[ND-HFD], and 4-4[HFD-ND] groups. I estimated the peak phase from the daily rhythm of bioluminescence expressed using the single cosinor procedure program. The peak phase of the liver rhythm in the 4-4[HFD-ND] group was advanced compared with that in the 4-4[ND-ND] and 4-4[ND-HFD] groups (Figure 2.6B). The phases of the liver clock in the 2-2[HFD-ND], 4-4[HFD-ND], and 8-8[HFD-ND] groups were advanced compared with that in the 4-4[ND-HFD] group (Figure 2.6C). The phase of the liver clock in the 2-12[HFD-ND] group was similar to that in the 4-4[ND-HFD] group (Figure 2.6D). These results suggest that to maintain the calorie intake during the active phase higher than that during the resting phase

would not shift the phase of the liver clock.

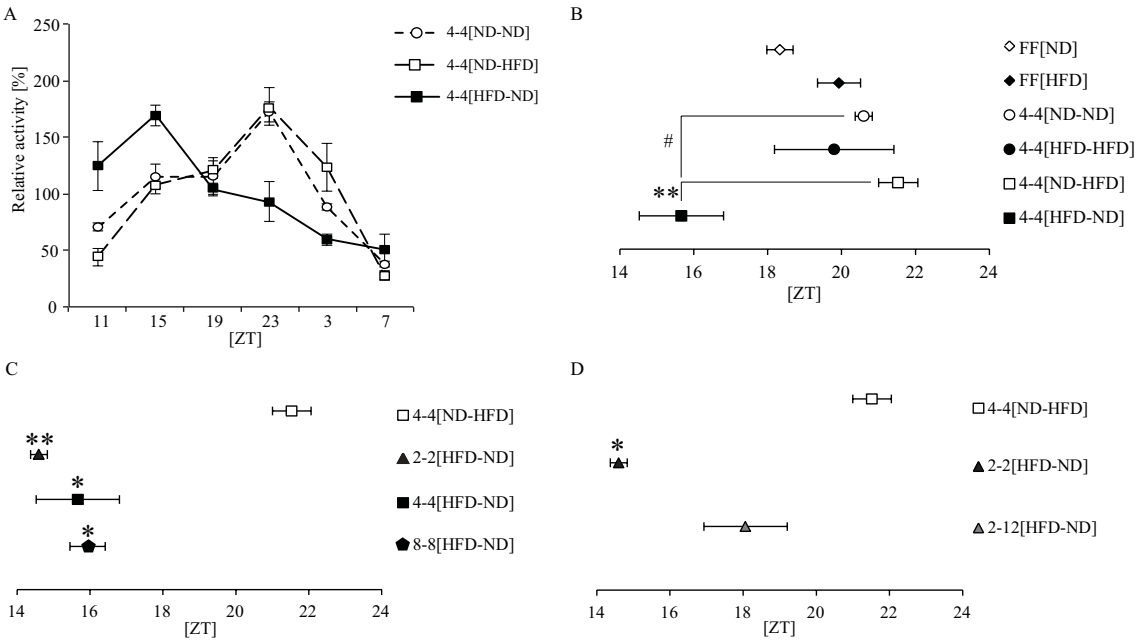

Figure 2.6 *In vivo* monitoring system for measuring PER2 expression rhythms in the mouse liver under each feeding treatment (Experiment 2.5)

(A) Analyzed data of PER2::LUC bioluminescence rhythms of individual livers in the 4-4[ND-ND], 4-4[ND-HFD], and 4-4[HFD-ND] groups. (B) Average peak phase of PER2::LUC rhythms in the liver under the same experimental treatments as experiment 2.1. (C) Average peak phases of PER2::LUC rhythms in the liver under the same experimental treatments as experiment 2.2. Data in the 4-4[ND-HFD] and 4-4[HFD-ND] groups are the same as those in the 4-4[ND-HFD] and 4-4[HFD-ND] groups in Figure 2.6B. (D) Average peak phase of PER2::LUC rhythms in the liver under the same experimental treatments as experiment 2.4. Data in the 4-4[ND-HFD] and 2-2[HFD-ND] groups are the same as the data in the 4-4[ND-HFD] group in Figure 2.6B and in the 2-2[HFD-ND] group in Figure 2.6C. Data are presented as the mean ± SEM, n = 3 for each feeding treatment. * $p < 0.05$, ** $p < 0.01$ vs. 4-4[ND-HFD] (Tukey-Kramer test). # $p < 0.05$ vs. 4-4[ND-ND] (Tukey-Kramer test).

2.4 Discussion

In this chapter, I clarified that the effects of RF duration on obesity are stronger than the effects of feeding pattern. Contrary to my hypothesis, I found that a short RF duration had a stronger effect on obesity than a longer RF duration.

I initially hypothesized that body weight gain might depend on feeding pattern. Accordingly, I expected that body weights of mice in the [HFD-ND] group would be more increased than those of mice in the [ND-HFD] group, because the consumption of lipid is difficult but the accumulation of lipid is easy during the resting phase. In experiment 2.1, body weights and visceral fat volumes in the 4-4[HFD-ND] group were similar to those in the 4-4[ND-HFD] group. In experiment 2.2, I observed that body weights and visceral fat volumes in the 8-8[HFD-ND] group were significantly higher than those in the 8-8[ND-HFD] group. On the other hand, body weights and visceral fat volumes in the 2-2[HFD-ND] and 4-4[HFD-ND] groups were similar to those in the 2-2[ND-HFD] and 4-4[ND-HFD] groups, respectively. Hatori et al. (2012) indicated that 8-hour RF with a HFD during the active phase caused normal body weight gain, and Sherman et al. (2012) reported that 4-hour RF with a HFD during the resting phase suppressed body weight gain more strongly than FF with a HFD. However, 12-hour RF with a HFD during the resting phase increased body weight gain (Arble et al., 2009), and eating a HFD during the latter portion of the active phase (ZT 20-24) was associated with multiple cardiometabolic syndromes (Bray et al., 2010). Wang et al. (2013) reported that consuming a HFD in the latter portion of the resting phase (ZT 10.5-11.5) affected the circadian clock in the liver and increased triglyceride content in mice. Body weights of rats fed in the middle and end of active phase increased more rapidly than those of rats fed in the beginning

and middle of active phase (Wu et al., 2011). Taken together, these results suggest that 4 hours is the optimal duration to suppress the effect of HFD on obesity. In other words, HFD does not always increase body weight and visceral fat volume, even if the HFD is consumed during the resting phase, when an adequate calorie intake is eaten within an adequate duration.

In my second hypothesis, I hypothesized that body weight gain might depend also on RF duration. Therefore, I anticipated that body weights in the 2-hour RF groups might be less increased than that in the other groups. As noted above, 4-hour RF duration was the optimal duration, and I added 2- and 8-hour RF treated mice as models of eating disorders. Increases in body weights and visceral fat volumes were higher in the 2-hour RF groups than in the 4-hour RF groups (Figures 2.3C and 2.3D), suggesting that a too short RF duration caused obesity. Therefore, I assumed that the 2-hour RF groups might be models of speed-eating habits. Previous studies in humans suggested an association between eating speed and the tendency to be overweight or obese (He et al., 2000; Sugimori et al., 2004; Otsuka et al., 2006). However, Ochiai et al. (2013) indicated that the eating speeds of individuals are difficult to assess objectively, because the information is obtained from self-reports. In experiment 2.3, calorie intake in the 2-hour RF groups was similar to that in the 4-hour RF groups, although the RF duration in the 2-hour RF groups was half of that in the 4-hour RF groups (Figure 2.4B). Mice in the 2-hour RF groups got more calories during the initial hour of RF than mice in the 4-hour RF groups (Figure 2.4C). Taking these results into consideration, I measured postprandial blood glucose levels in the 2- and 4-hour RF groups after each RF. Postprandial blood glucose levels in the 2-hour RF groups were more increased than those in the 4-hour RF groups. Taken together, these results suggested that speed-eating habits might impair glucose tolerance and

might cause obesity. My results in chapter 2 confirmed the findings from studies in humans, which indicated that speed-eating habits have a negative effect with regard to body weight gain, accumulation of visceral fat, and obesity.

Many studies in mice have shown that RF entrained the circadian rhythm in the liver but not in the SCN (Hara et al., 2001; Schibler et al., 2003). Therefore, the present results indicated that RF with a HFD during the resting phase, similar to night eating syndrome (NES) in humans, shifts the phase of the expression rhythms of clock genes in the liver, subsequently resulting in phase mismatches of clock gene expression rhythms between the SCN and the liver. Accordingly, I hypothesized that this situation is similar to jet lag. Shifting of the LD cycle, which is a model of jet lag, was found to cause a desynchronization of the body and SCN clocks, subsequently leading to obesity (Karatsoreos et al., 2011; Filipski et al., 2006). I observed that in the 2-12[HFD-ND] group, visceral fat volumes were low and the clock phase in the liver was not advanced compared with those in the 2-2[HFD-ND] group (Figures 2.5E and 2.6D). Taken together, these results suggest that this phase mismatch of clock gene expression may enhance the effects of RF with a HFD during the resting phase on body weight gain. Moreover, I demonstrated that the effects of eating habits on obesity would be stronger than those of the mismatch between central and peripheral clocks, because body weight and visceral fat in the 2-hour RF groups were increased regardless of feeding patterns.

In conclusion, I demonstrated that unhealthy eating habits, such as speed-eating habits, might be important factors in contributing to increase in body weight and the accumulation of visceral fat. Moreover, HFD meals during the resting phase increased the risks of body weight increase, accumulation of visceral fat, and shift of the circadian rhythm in the

liver. However, my results also indicated that these risks are decreased when calorie intake during the resting phase is lower than that during the active phase. Taken together, the mismatch between the central and peripheral clocks may contribute to the development of obesity; however, eating habits are a more important factor in causing obesity than the mismatch between the central and peripheral clocks.

Chapter 3. Effects of disrupted feeding rhythm on depressive-like behavior

3.1 Introduction

The central clock regulates the secretion rhythms of hormones, including leptin, orexin, and ghrelin, and also modulates appetite (Kalsbeek et al., 2001; Zhang et al., 2004; Kirsz & Zieba, 2012). On the other hand, the timing of food intake as well as the composition of the food are important entrainment factors for peripheral clocks (Hirao et al., 2010; Kuroda et al., 2012; Tahara & Shibata, 2016). Taken together, previous studies suggested that the circadian clock system closely interacts with the appetite rhythm. However, the circadian clock system in eating rhythm disorders, including NES, has not been yet analyzed. Patients with NES have episodes of midnight eating with consciousness (Inoue, 2015). NES is diagnosed by specific criteria (Allison et al., 2010), and is listed in the *Diagnostic and Statistical Manual of Mental Disorders* 5th edition. One of the characteristics of patients with NES is a decline in their mood during the evening and night, which is defined as time-specific depression symptoms. The time-specific depression symptoms are in contrast to depression symptoms in patients with depression, which usually occur in the morning (Birketvedt et al., 1999). Taken together, midnight eating, which is defined as a disrupted eating rhythm, might be associated with time-specific depression symptoms.

In this chapter, I focused on the time-specific depression symptoms observed in patients with NES and hypothesized that the disrupted eating rhythm, similar to the eating rhythm of patients with NES, might lead to time-specific depression symptoms. Previous

studies have applied homozygous *Clock* mutant mice, prostanoid receptor EP3R knock-out mice, and histamine H1 receptor knock-out mice as models of changed/delayed feeding rhythm (Turek et al., 2005; Sanchez-Alavez et al., 2007; Masaki et al., 2004). I did not analyze the effects of a disrupted feeding rhythm on time-specific depressive-like behavior using such mutant and/or knock-out mice. The reason was because the gene mutations and knock-out themselves might affect depressive-like behavior (Li et al., 2015). Furthermore, a previous study used RF during the resting phase in rhesus monkeys (Sullivan et al., 2005). However, I did not analyze the effects of a disrupted feeding rhythm on time-specific depressive-like behavior using this feeding treatment. The reason was that RF and acute forced fasting themselves might affect the depressive-like behavior (Li et al., 2014). Taken together, I first needed to establish a new NES model using wild-type mice without a forced-fasting period. In chapter 2, I observed that mice ate a HFD at ZT 5 in the 2-2[HFD-ND], 2-6[HFD-ND], and 2-12[HFD-ND] groups (Haraguchi et al., 2014). Accordingly, I applied RF with a HFD for a short duration at ZT 5 and FF with a ND, as a new NES model (Figure 3.1A). I assumed that this feeding treatment would imitate the characteristics of patients with NES, i.e., a delayed phase of the circadian eating pattern (Allison & Stunkard, 2005).

Dysfunction in the monoamine systems of serotonin (5-hydroxytryptamine; 5-HT) and norepinephrine (NE) are expected to lead to depression symptoms, because selective serotonin reuptake inhibitors (SSRIs), serotonin norepinephrine reuptake inhibitors, and other methods of monoamine reuptake work as antidepressants (Kennedy et al., 2001; Anderson et al., 2000; Mulrow et al., 1999). Previous studies in mice showed that the 5-hydroxyindole acetic acid (5-HIAA)/5-HT ratio (indicates the 5-HT metabolic rate; 5-HIAA is one of the 5-HT

metabolites) was increased in a mouse model of depression (Kageyama et al., 2010), and antidepressants decrease the 5-HIAA/5-HT ratio in the hippocampus (Li et al., 2007). Another study showed an association between hypofunction of the noradrenergic system and depression symptoms, and suggested that the effect of some antidepressants on NE and one of the NE metabolites (3-methoxy-4-hydroxyphenylglycol; MHPG) (Brunello, 2003). Clinical studies in humans indicated that SSRIs and tricyclics, such as escitalopram, sertraline, and topiramate, improved depression symptoms in about half of the participants with NES (O'Reardon et al., 2004; Allison et al., 2013). A study in mice suggested that depressive-like behavior were caused by long-term FF with a HFD, which was considered as an unhealthy food (Aslani et al., 2015), and a study in humans indicated that healthy food, including fruit, vegetables, and olive oil, would reduce the risk of depression symptoms (Martínez-González & Sánchez-Villegas, 2016). However, the effects of disrupted eating rhythms on depression symptoms and monoamine systems has not yet been investigated.

In this chapter, I had four main aims. First, I aimed to establish a new NES model using wild-type mice without a forced fasting period. I made a mouse model of disrupted feeding rhythm similar to the eating pattern of patients with NES (NES model). Second, I aimed to analyze the association between disrupted eating rhythms and time-specific depression. I analyzed the effect of a disrupted feeding rhythm on time-specific depressive-like behavior using the forced swimming test (FST), which was established for the analysis of depressive-like behavior (Porsolt et al., 1977). Third, I aimed to elucidate the cause of time-specific depressive-like behavior from the perspectives of the monoamine system and circadian clock system. Moreover, I measured monoamine levels in the hippocampus before and after the FST,

and analyzed stress reactivities of the monoamine system. Last, I analyzed the effects of desipramine on the time-specific depressive-like behavior caused by NES feeding patterns.

Consent from all authors has been obtained.

3.2 Materials and Methods

3.2.1 Animals

Eight-week-old ICR mice and PER2::LUC knock-in mice were housed in the animal room under the same room and feeding conditions as described in chapter 2, until the time of the experiments. Female mice were used in most of the experiments, because the criteria for NES were established by analyzing eating patterns in a group of obese women (Stunkard et al., 1955). The procedures conformed to the "Fundamental Guidelines for Proper Conduct of Animal Experiments and Related Activities in Academic Research Institutions" (published by the Ministry of Education, Culture, Sports, Science and Technology, Japan) and were approved by the Committee for Animal Experimentation at Waseda University (permission no. 2016-A065).

3.2.2 Diets

Mice were fed with a ND and/or a HFD during the experiments. HFD consisted of the AIN-93M formula diet (Oriental Yeast Co. Ltd., Tokyo, Japan) combined with lard oil (Sigma-Aldrich, MO, USA) at a ratio of 4:1 (w/w). In HFD, approximately 45% of the calories were from fat.

3.2.3 Feeding treatments

Mice were divided into 2 groups, namely, the control and NES model groups. All mice were individually housed in cages under FF with a ND and water. In addition, in the NES model group, RF with a HFD for a short duration was started at ZT 5. The feeding pattern in the

NES model group emulated the eating patterns of patients with NES. Body weights and food intake were measured every week. Food intake was expressed as kcal/mouse/day.

3.2.4 Locomotor activity analysis

Each mouse was housed in individual cages during the experiments. Locomotor activity was monitored using an infrared radiation sensor (SE-10; Akizuki Denshi Tsusho Co. Ltd., Tokyo, Japan) and analyzed by CLOCKLAB software (Actimetrics, IL, USA). The relative locomotor activity every hour was estimated using the following formula: (counts per hour/counts per day) × 100 (%).

3.2.5 *In vivo* monitoring protocol and data analysis

The protocol and analysis method for the *in vivo* monitoring system are as described in chapter 2, except for the timing of the measurements. Images were taken at 8 and 10 minutes after D-luciferin injection in the dorsal-up position for the kidney and in the ventral-up position for the liver, respectively. Images were obtained six times a day (ZT 7, 11, 15, 19, 23, and 3).

3.2.6 Forced swimming test (FST)

The method of the FST was first established by Porsolt et al. (1977), and then improved in other studies (Porsolt et al., 1979; Borsini et al., 1989; Matsuno et al., 1996; Lin et al., 2014). Mice were set in a polymethylpentene cylinder (diameter 137 mm; height 200 mm) filled with water at about 25 °C to a depth of approximately 150 mm for 15 minutes as a pre-test. After 24 hours, mice were placed in the same field for 6 minutes, and their activities were

recorded for 6 minutes by video camera. Immobility time was measured for the last 4 minutes of the 6 minutes by observers who had no information about the feeding treatments and the order of the mice. Immobility was defined as when mice stopped swimming and remained floating in the water.

3.2.7 High performance liquid chromatography-electrochemical detection (HPLC-ECD)

Levels of 5-HT, 5-HIAA, NE, and MHPG in the hippocampus were measured by HPLC-ECD (HTEC 500; Eicom, Kyoto, Japan), following the protocol used in previous studies (Tahara et al., 2015; Sasaki et al., 2016). In experiment 3.7, mice were maintained under each feeding treatment for 4 weeks before sacrifice. At ZT 1 and 13, mice were sacrificed with isoflurane without or after the FST, and the hippocampus was removed for the measurements. Perchloric acid (0.2 M, including 100 μM ethylenediaminetetraacetic acid (EDTA)・2Na) containing 20 ng of isoproterenol was added to all samples. Samples were homogenized using a micro-homogenizer before being centrifuged at 15,000 rpm at 4 °C for 15 minutes. The supernatants of all samples were collected and filtered using a 0.45-μm filter (low protein-binding durapore [Poly Vinylidene Di-Fluoride] membrane; Merck KGaA, Darmstadt, Germany). Subsequently, monoamines in each 20 μL sample were quantified simultaneously using HPLC-ECD with the following conditions: 85% of the transfer phase was composed of 0.1 M acetate-citric acid buffer (pH 3.5), including 5 mg/L EDTA・2Na, 190 mg/L 1-octanesulfonic acid sodium salt, and 15% methanol. The velocity of the flow was 500 μL/minute. The column temperature was 25 °C and the applied voltage was +750 mV versus Ag/AgCl. The data were analyzed using EPC-300 software (Eicom).

3.2.8 Drug treatments

Desipramine (10 mg/kg, Sigma-Aldrich, dissolved in saline) was administered 30 minutes prior to the FST and was injected intraperitoneally. Mice in the saline group were injected with saline.

3.2.9 Statistical analysis

All values are expressed as the mean ± SEM. Statistical analysis was conducted using GraphPad Prism version 6.03 (GraphPad software, CA, USA). Estimation of whether the data distribution was normal or not was performed using the D'Agostino-Pearson normality test, Kolmogorov-Smirnov test, or one-sample *t*-test. Subsequently, whether the data variation was equal or biased was estimated using the *F*-value test or Bartlett test. Parametric analysis was performed by the Student *t*-test or one-way ANOVA with the Tukey multiple comparison test, and non-parametric analysis was estimated by the Mann-Whitney test or Kruskal-Wallis test with Dunn multiple comparison test. Two-way ANOVA with the Tukey multiple comparison test was performed only when the data distribution was normal and the variation was equal. In other cases, the Student *t*-test, one-way ANOVA with the Tukey multiple comparison test, Mann-Whitney test, or Kruskal-Wallis test with Dunn multiple comparison test was performed at each time point and within the same group.

3.3 Results

3.3.1 Five-minute RF with a HFD is the optimal feeding treatment for imitating the eating patterns of patients with NES (Experiment 3.1)

To establish a NES model, mice in the NES model group were maintained under RF with a HFD from ZT 5 and FF with a ND (Figure 3.1A). This feeding treatment was considered to mimic eating patterns of patients with NES, which is characterized by a delayed circadian eating pattern (Allison & Stunkard, 2005). In chapter 2, I showed that mice ate more than 30% of their total calorie intake from a HFD in the 2-2[HFD-ND], 2-6[HFD-ND], and 2-12[HFD-ND] groups (Haraguchi et al., 2014). To decide on the RF duration, I measured the effects of some RF durations on calorie intake and on relative locomotor activity rhythm, and sought a feeding treatment that maintained calorie intake from a HFD at approximately 25% of the total calorie intake, and which also affected relative locomotor activity rhythm. Compared with the control group, mice in the NES model group had increased relative locomotor activity levels during the middle of the resting phase, when RF with a HFD was stopped after mice were maintained under each feeding treatment for more than 2 weeks. Relative locomotor activity levels during the middle of the resting phase in the NES model group were higher than those in the control group (Figures 3.1B and 3.1C). Body weights in the NES model group were greater than in the control group (Figure 3.1D). In the NES model group, calorie intake from a ND was decreased compared with that in the control group, because mice in the NES model group received a HFD during RF. Total calorie intake in the NES model group was higher than that in the control group when the RF duration was 30 and 60 minutes. Total calorie intake in both groups was similar to each other when the RF duration was less than 15 minutes (Figures 3.1E

and 3.1F). Under RF with a HFD for 15-60 minutes, mice in the NES model group received more than 25% of their total calorie intake from a HFD. Moreover, their calorie intake from a HFD was approximately 25% of their total calorie intake when RF duration was 5 minutes (Figure 3.1G). These results suggested that 5-minute RF duration would be sufficient to establish a new NES model mouse.

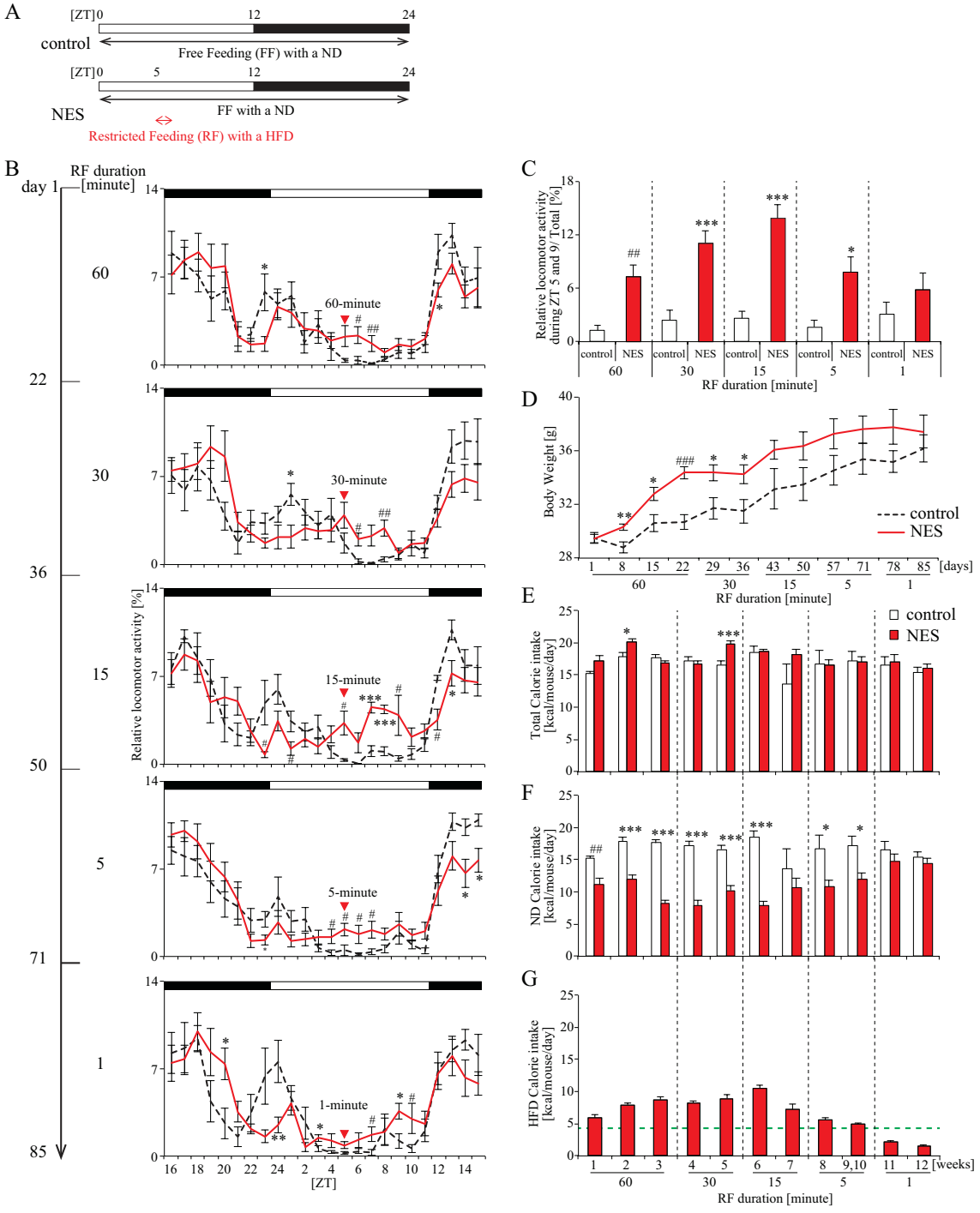

Figure 3.1 Effects of different durations of RF with a HFD at ZT 5 and FF with a ND on relative locomotor activity rhythm, body weight, and calorie intake (Experiment 3.1)

(A) Feeding treatments. Mice in the control group were housed under FF with a ND, and mice in the NES group were maintained under FF with a ND and RF with a HFD at ZT 5. (B)

Relative locomotor activity rhythms at each RF duration (60, 30, 15, 5, and 1 minute). Red triangles represent the start of RF. Open and closed bars indicate the resting and active phases, respectively. (C) Total relative locomotor activities between ZT 5 and 9. (D) Body weights. (E-G) Average calorie intake of total (E), ND (F), and HFD (G) under each feeding treatment. Green dashed line indicates the approximately 25% level of total calorie intake by mice in the NES model group. Data are presented as the mean ± SEM (control group, n = 6; NES model group, n = 8). * $p < 0.05$, ** $p < 0.01$, *** $p < 0.001$ vs. the control group (Student *t*-test). # $p < 0.05$, ## $p < 0.01$, ### $p < 0.001$ vs. the control group (Mann-Whitney test).

3.3.2 Five-minute RF with a HFD and FF with a ND increased relative locomotor activity and calorie intake during the resting phase up to week 12 (Experiment 3.2)

To analyze the long-term effects of 5-minute RF with a HFD and FF with a ND on feeding pattern, body weight, and relative locomotor activity rhythm, two groups of mice were maintained for three months (Figure 3.2A). In the NES model group, mice with a HFD were fed for 1 hour in the initial week to be accustomed to the RF feeding treatment. Both groups had similar amounts of total calorie intake, and mice in the NES model group consistently received about 25% of their total calorie intake during RF with a HFD from week 4 (Figures 3.2B-3.2D). The NES model group had lower calorie intake during the active phase and higher calorie intake during the resting phase than the control group at week 5 (Figure 3.2H). Relative locomotor activity levels during the middle of the resting phase in the NES model group were higher than those in the control group. Moreover, the periods of low relative locomotor activity in the NES model group were short and intermittent (Figures 3.2E and 3.2G). Body weights in the NES model group tended to be higher than those in the control group, but there was no statistically significant difference (Figure 3.2F). These results indicate that the effect of 5-minute RF with a HFD and FF with a ND on feeding patterns and relative locomotor activity rhythms are stable from week 4.

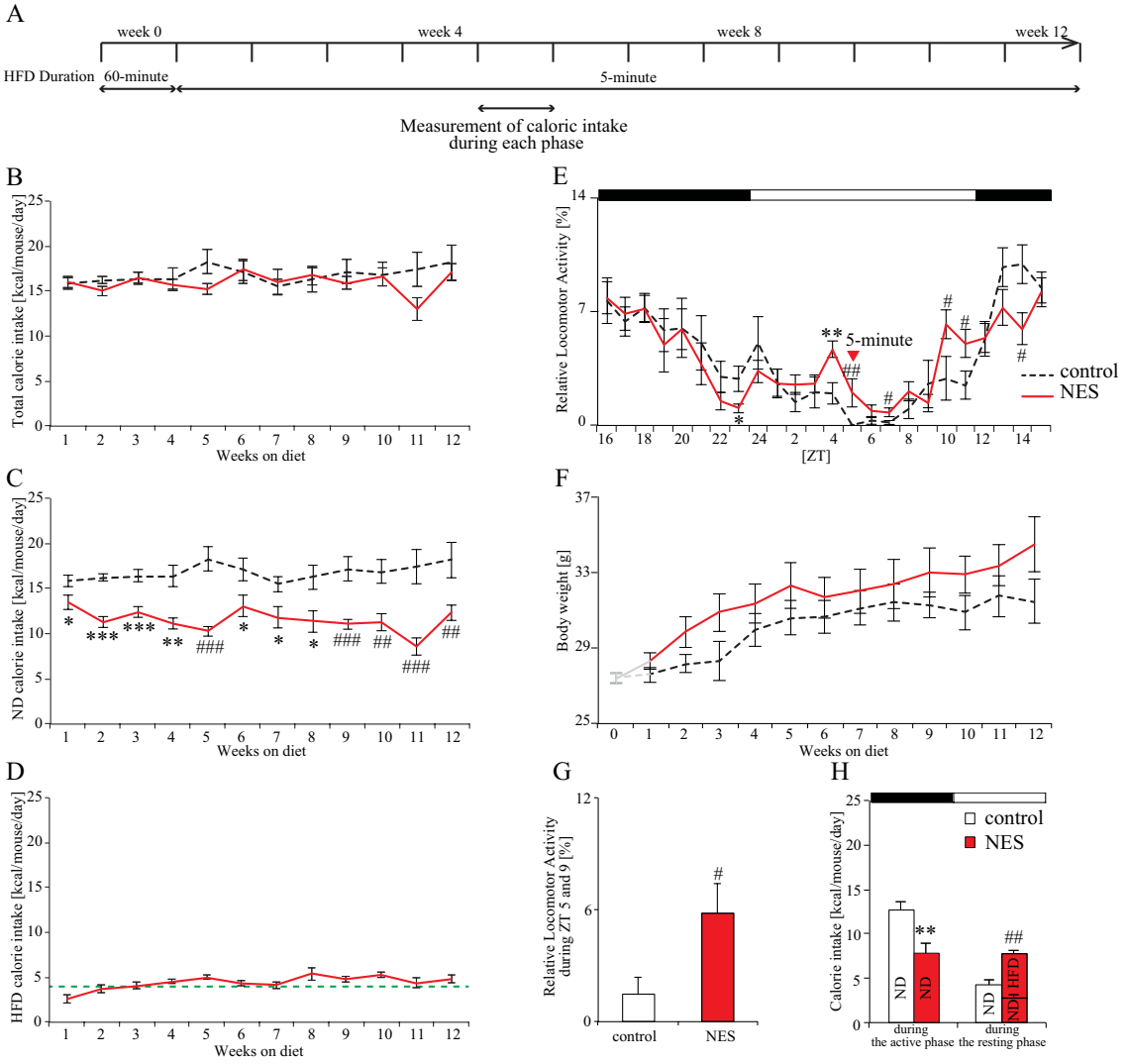

Figure 3.2 Effects of 5-minute RF with a HFD at ZT 5 and FF with a ND on relative locomotor activity rhythm, body weight, and calorie intake (Experiment 3.2)

(A) Experimental treatment. (B-D) Average calorie intake of total (B), ND (C), and HFD (D) under each feeding treatment. Green dashed line indicates the approximately 25% level of total calorie intake of mice in the NES model group. (E) Relative locomotor activity rhythms of each group. Red triangle represents the start of RF. Open and closed bars indicate the resting and active phases, respectively. (F) Body weights. Gray lines indicate mice under habituation. (G) Total relative locomotor activity between ZT 5 and 9. (H) Calorie intake during each phase

from a ND and a HFD. The diets of each group (ND or HFD) are indicated in every bar. Data are presented as the mean ± SEM (n = 8). * $p < 0.05$, ** $p < 0.01$, *** $p < 0.001$ vs. the control group (Student *t*-test). # $p < 0.05$, ## $p < 0.01$, ### $p < 0.001$ vs. the control group (Mann-Whitney test).

3.3.3 FF with a ND is an optimal control treatment for the NES model group (Experiment 3.3)

To confirm whether the FF treatment was an optimal control feeding treatment for the NES model group, I performed further experiments. I added the NES-ZT5-ND group, which was maintained under 5-minute RF with a ND at ZT 5 and FF with a ND, and the NES-ZT17-HFD group, which was maintained under 5-minute RF with a HFD at ZT 17 and FF with a ND, to the control and NES model (NES-ZT5-HFD) groups (Figure 3.3A). Total calorie intake in the four groups was similar, whereas ND calorie intake in the NES-ZT17-HFD group was significantly lower than that in the other groups (Figure 3.3B). Body weights in the NES-ZT5-ND group were higher than those in the control and NES-ZT17-HFD groups, and lower than those in the NES-ZT5-HFD group; however, there were no significant differences in body weights at week 5 (Figure 3.3C). Relative locomotor activity rhythms in the control and NES-ZT5-ND groups were similar. In the NES-ZT5-HFD group, relative locomotor activity levels at ZT 5 were higher than in the other groups (Figure 3.3D). These results indicate that FF with a ND might be an optimal control feeding treatment for the NES model group.

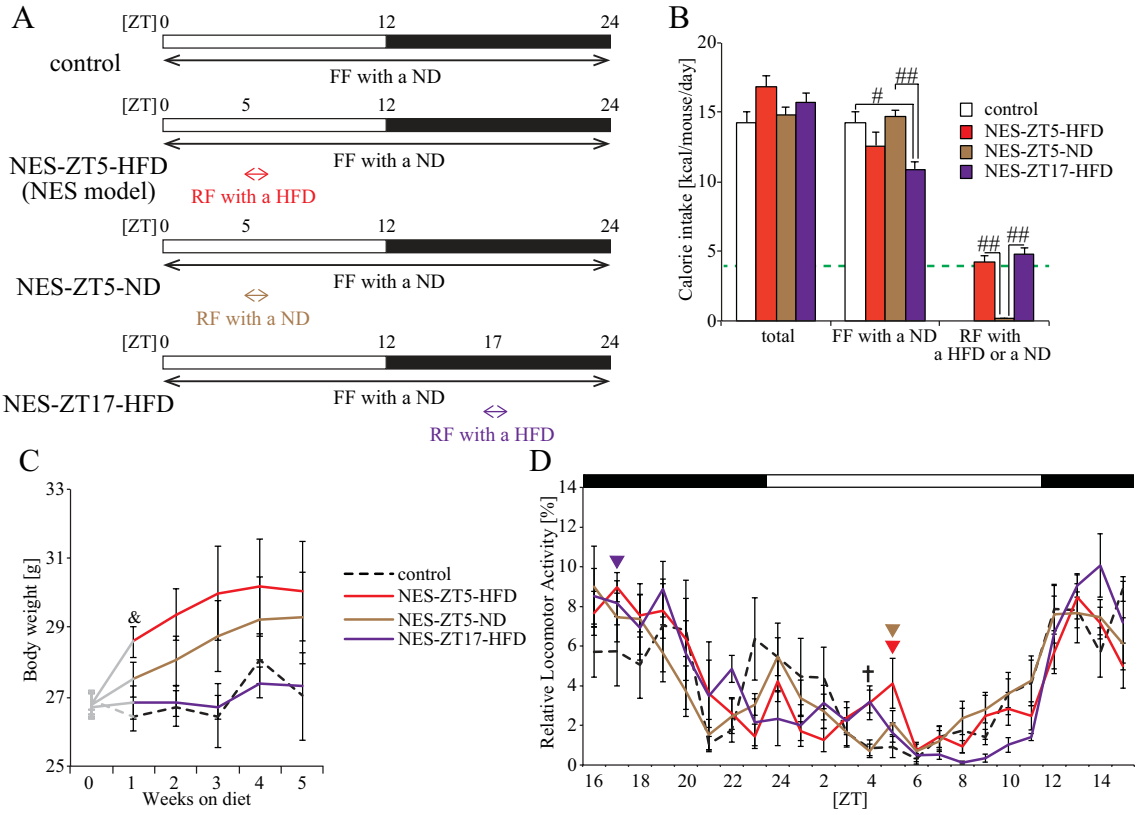

Figure 3.3 Effects of 5-minute RF with a HFD at ZT 17 or a ND at ZT 5 on relative locomotor activity rhythms, body weights, and calorie intake (Experiment 3.3)

(A) Feeding treatments. (B) Average calorie intake of total, FF with a ND, and RF with a HFD or a ND under each feeding treatment. Green dashed line indicates the approximately 25% level of total calorie intake of mice in the NES-ZT5-HFD and NES-ZT17-HFD groups. (C) Body weights. Gray lines indicate mice during habituation. (D) Relative locomotor activity rhythms under each feeding treatment. Red and purple triangles represent the start of RF with a HFD and brown triangle represents the start of RF with a ND. Open and closed bars at the top indicate the resting and active phases, respectively. Data are presented as the mean ± SEM (n = 7). † $p < 0.05$ vs. the NES-ZT5-ND group (one-way ANOVA with Tukey multiple comparison test). # $p < 0.05$, ## $p < 0.01$ (Kruskal-Wallis test with Dunn multiple comparison test).

3.3.4 Five-minute RF with a HFD and FF with a ND increased immobility times only at ZT 1, an early time point in the resting phase (Experiment 3.4)

To analyze the effects of 5-minute RF with a HFD and FF with a ND on depressive-like behavior, I analyzed immobility times in the FST of mice fed under each feeding treatment for several weeks. Experiment 3.2 demonstrated that feeding patterns and relative locomotor activity rhythms in the NES model group were stable from week 4. Accordingly, I first analyzed immobility times at ZT 1 and 13 using different mice after each feeding treatment for 4 weeks. As a result, immobility times at ZT 1 in the NES model group were increased to a greater degree than those in the control group (Figure 3.4A). Subsequently, I observed immobility times at six different ZTs, with 2-week intervals of the FST. This interval was necessary for the removal of the effects of the previous FST on immobility time. I divided the control and NES groups into 2 groups. In one group, I performed the FST at ZT 5 in week 4, at ZT 17 in week 7, and at ZT 1 in week 10. In another group, I performed the FST at ZT 9 in week 4, at ZT 21 in week 7, and at ZT 13 in week 10. The results showed that immobility times in the NES model group were increased only at ZT 1 (Figure 3.4B), suggesting that 5-minute RF with a HFD and FF with a ND prolong immobility times at a specific time, namely, ZT 1. I made another NES model group to verify reproducibility of the results. I confirmed that 5-minute RF with a HFD and FF with a ND prolongs immobility time at ZT 1 when mice were treated with 5-minute RF for a long time (12 weeks) (Figure 3.4C). These results suggest that 5-minute RF with a HFD and FF with a ND would prolong immobility time only at ZT 1, which was referred to as time-specific depressive-like behavior.

Furthermore, I analyzed immobility times in the NES-ZT5-ND and NES-ZT17-HFD

groups, and found that they were similar to those in the control group (Figures 4.4D and 4.4E). These results indicated that FF with a ND is an optimal control feeding treatment for the NES model group.

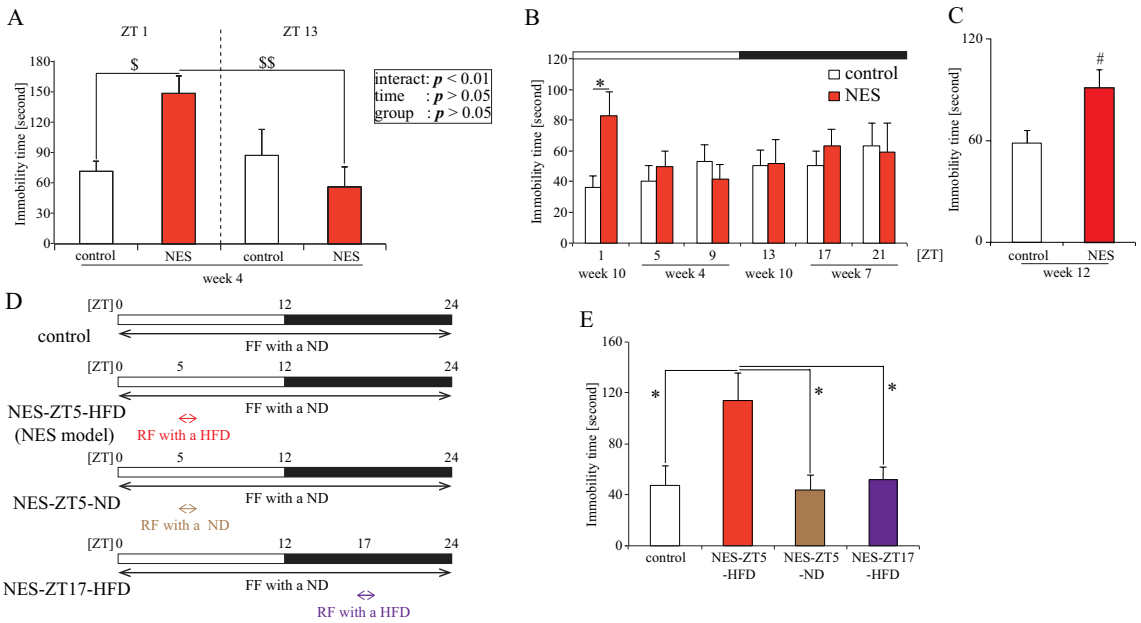

Figure 3.4 Effects of 5-minute RF with a HFD at ZT 5 and FF with a ND on immobility time (Experiment 3.4)

(A) Immobility times at ZT 1 and 13, after each feeding treatment for 4 weeks (n = 8). The results of two-way ANOVA are presented on the right side of the graph. (B) Immobility times at ZT 1, 5, 9, 13, 17, and 21. FSTs were performed after each feeding treatment for 4 weeks, and the interval between each FST was 2 weeks (control group, n = 6; NES model group, n = 7). The FST at ZT 5 and 9 were performed in week 4, the FST at ZT 17 and 21 were performed in week 7, and the FST at ZT 1 and 13 were performed in week 10. Open and closed bars indicate the resting and active phases, respectively. (C) Immobility times at ZT 1, after each feeding treatment for 12 weeks (n = 8). (D) Feeding treatments. (E) Immobility times at ZT 1 after maintaining mice on each feeding condition for 4 weeks (n = 7). Data are presented as the mean ± SEM. * $p < 0.05$ vs. the control group (Student *t*-test). # $p < 0.05$ (Mann-Whitney test). † $p < 0.05$ (one-way ANOVA with Tukey multiple comparison test). $ $p < 0.05$, $$ $p < 0.01$ (two-way ANOVA with Tukey multiple comparison test).

3.3.5 Five-minute RF with a HFD and FF with a ND affected relative locomotor activity rhythm, calorie intake, and immobility time regardless of sex, but not two-minute RF (Experiment 3.5)

In experiment 3.4, I clarified that immobility times in the NES-5min group were longer than in the control group. Therefore, to determine whether the act of taking a meal during the resting phase or taking a large amount of calories during the resting phase is a more important factor for causing time-specific depressive-like behavior, I prepared three groups. Mice in the control group were maintained under FF with a ND, mice in the NES-5min group were fed 5-minute RF with a HFD and FF with a ND, and mice in the NES-2min group were fed 2-minute RF with a HFD and FF with a ND. The NES-5min group was considered to be the optimal feeding treatment for the NES model group, and the NES-2min group was considered to be a group receiving low calorie intake from a HFD. ND calorie intake in the control and NES-2min groups was similar, and that in the NES-5min group was lower. HFD calorie intake in the NES-5min group was significantly increased compared with that in the NES-2min group (Figure 3.5A). Similar to previous results (Figure 3.4), immobility times at ZT 1 in the NES-5min group were significantly prolonged compared with those in the other groups (Figure 3.5B). I observed relative locomotor activity rhythms in each group (Figure 3.5C), and confirmed that relative locomotor activity levels during the middle of the resting phase in the NES-5min group were higher than those in the other groups (Figure 3.5D). Furthermore, I confirmed whether NES feeding patterns would cause male mice to show time-specific depressive-like behavior. I observed that the results of calorie intake, body weight, and relative locomotor activity rhythm were similar to those in female mice (Figures 3.6A-3.6D).

Immobility times at ZT 1 in the NES model group were significantly longer than those in the control group (Figure 3.6E). Taken together, these results suggest that the NES feeding patterns would prolong the immobility time at ZT 1 regardless of sex, and that time-specific depressive-like behavior are caused by the taking of a large amount of calories during the resting phase, and not by the action of taking a meal during the resting phase.

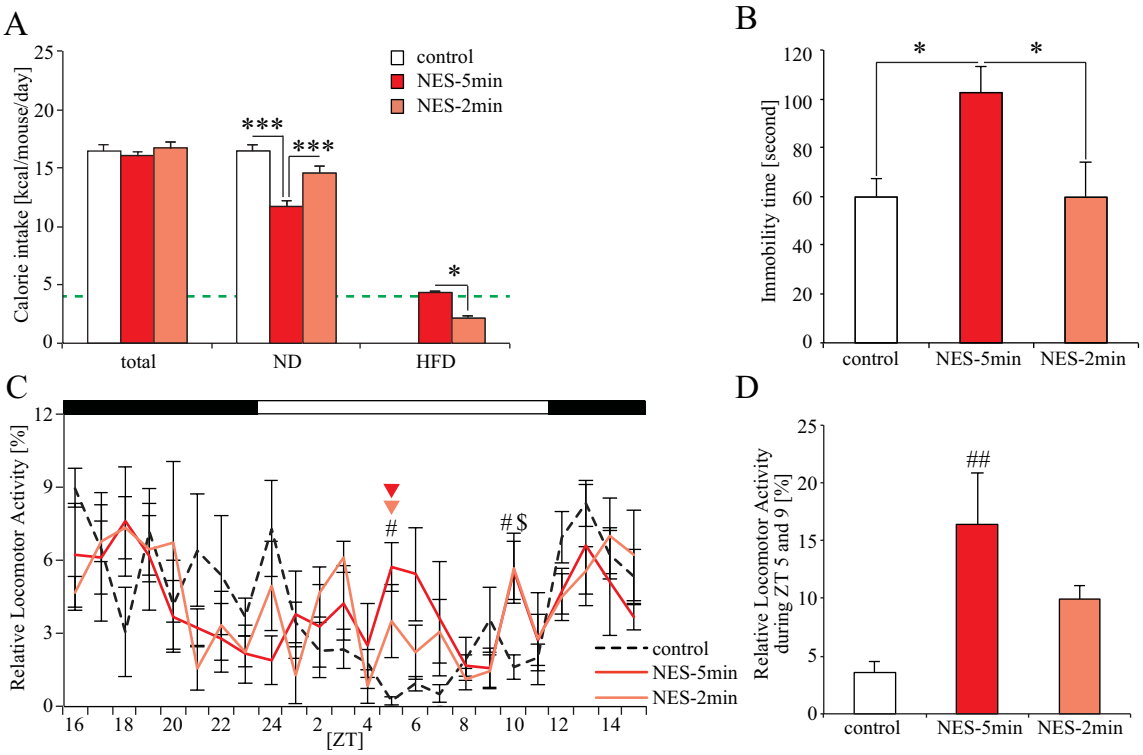

Figure 3.5 Effects of 5-minute and 2-minute RF with a HFD at ZT 5 and FF with a ND on calorie intake, relative locomotor activity rhythm, and immobility time at ZT 1 (Experiment 3.5)

(A) Average calorie intake of total, ND, and HFD under each feeding treatment. Green dashed line indicates the approximately 25% level of total calorie intake in mice in the NES-5min and NES-2min groups. (B) Immobility time at ZT 1. Data are presented as the mean ± SEM (control group, n = 6; NES-5min and NES-2min groups, n = 7). (C) Relative locomotor activity rhythms under each feeding treatment. Red and orange triangles represent the start timing of RF. Open and closed bars indicate the resting and active phases, respectively. (D) Total relative locomotor activity levels between ZT 5 and 9. Data are presented as the mean ± SEM (control group, n = 6; NES-5min and NES-2min groups, n = 4). * $p < 0.05$, *** $p < 0.001$ (one-way ANOVA with Tukey multiple comparison test). # $p < 0.05$, ## $p < 0.01$, NES-5min group vs. control group.

$ $p < 0.05$, NES-2min group vs. control group (Kruskal-Wallis test with Dunn multiple comparison test).

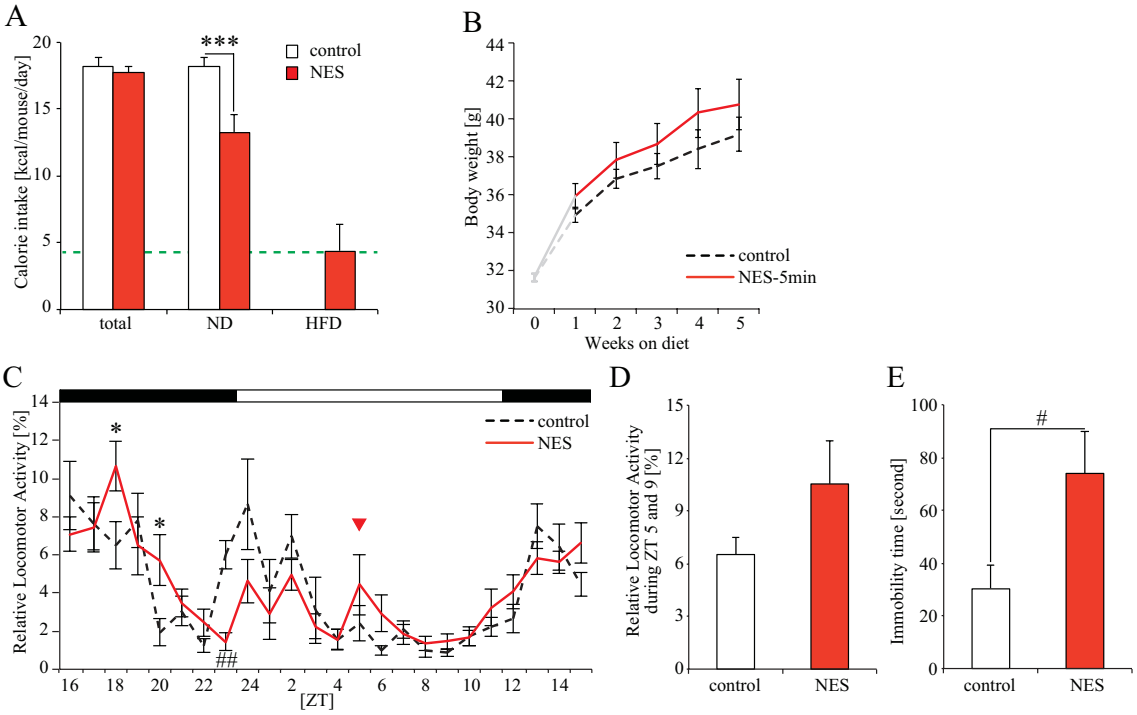

Figure 3.6. Effects of 5-minute RF with a HFD at ZT 5 on locomotor activity rhythm, body weight, calorie intake, and immobility time in male mice (Experiment 3.5)

(A) Average calorie intake of total, ND, and HFD under each feeding treatment. Green dashed line indicates the approximately 25% level of total calorie intake in mice in the NES model group. (B) Body weight. Gray lines indicate the weights of mice during habituation. (C) Relative locomotor activity rhythms under each feeding treatment. Red triangle indicates the start of RF with a HFD. Open and closed bars indicate the resting and active phases, respectively. (D) Total relative locomotor activities between ZT 5 and 9. (E) Immobility times at ZT 1 after maintaining mice under each feeding treatment for 4 weeks. Data are presented as the mean ± SEM (n = 8). * $p < 0.05$, *** $p < 0.001$ (Student *t*-test). # $p < 0.05$, ## $p < 0.01$ (Mann-Whitney test).

3.3.6 Five-minute RF with a HFD and FF with a ND affected the phase of peripheral clocks, but not two-minute RF (Experiment 3.6)

In experiment 3.5, I demonstrated that the taking of a large amount of calories during the resting phase might be an important factor for time-specific depressive-like behavior. A previous study indicated that the phases of peripheral clocks can be entrained also by the amount of calorie intake (Hirao et al., 2010). Therefore, to analyze the effects of the NES-5min and NES-2min feeding treatments on peripheral clocks, I observed bioluminescence rhythms in the kidney and liver using PER2::LUC knock-in mice and IVIS (Yoo et al., 2004; Tahara et al., 2012). I observed the peripheral clocks in the kidney and the liver using an *in vivo* monitoring system after each feeding treatment for 4 weeks. PER2 expression rhythms in the kidney and liver of the NES-5min group were advanced compared with those in the control and NES-2min groups (Figure 3.7). I demonstrated that immobility time in the NES-5min group was significantly longer than that in the NES-2min group (Figure 3.5B). Taken together, these results suggest that the amount of calorie intake during 5-minute RF, which would affect peripheral clocks, is an important factor in causing time-specific depressive-like behavior.

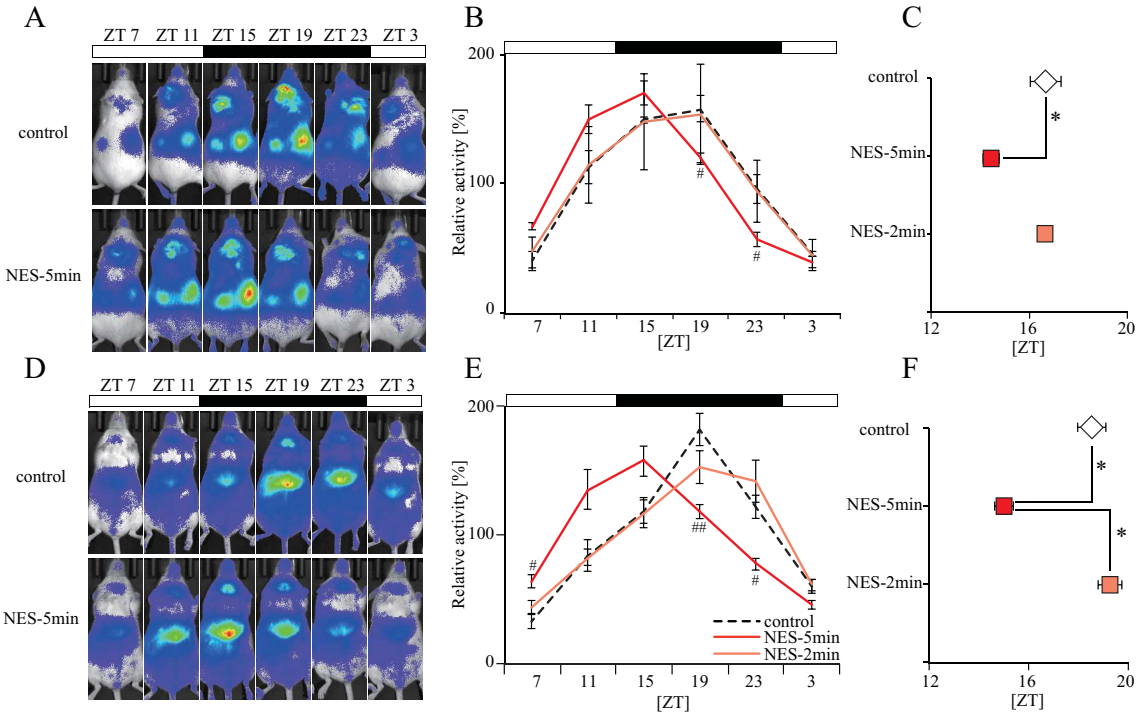

Figure 3.7 Effects of 5-minute and 2-minute RF with a HFD at ZT 5 and FF with a ND on peripheral clocks (Experiment 3.6)

(A-F) Representative images (A and D), analyzed wave forms (B and E), and peak phases (C and F) of *in vivo* PER2::LUC bioluminescence in the kidney (A-C) and the liver (D-F). Open and closed bars indicate the resting and active phases, respectively. Data are presented as the mean ± SEM (control group, n = 6; NES-5min group, n = 5; NES-2min group, n = 3). * $p < 0.05$ (one-way ANOVA with Tukey multiple comparison test). # $p < 0.05$, ## $p < 0.01$ (Kruskal-Wallis test with Dunn multiple comparison test).

3.3.7 Five-minute RF with a HFD and FF with a ND affected 5-HT levels and 5-HT metabolism in the hippocampus (Experiment 3.7)

To clarify the cause of the time-specific depressive-like behavior in the NES model group, I measured the 5-HT levels and 5-HIAA/5-HT ratios (metabolic rates) in the hippocampus by HPLC-ECD. Under no FST treatment (Figure 3.8A), the 5-HT and 5-HIAA levels showed similar levels in both the control and NES model groups (Figures 3.8B and 3.8C). The 5-HT levels and 5-HIAA/5-HT ratios in the NES model group showed significant differences between ZT 1 and 13, whereas those in the control group showed no significant differences (Figures 3.8C and 3.8D). Moreover, the 5-HIAA/5-HT ratios at ZT 1 in the NES model group were higher than in the control group (Figure 3.8D). A previous study suggested that the metabolic rates of monoamine in depression model mice were increased (Kageyama et al., 2010). Subsequently, I measured the 5-HT, 5-HIAA, and 5-HIAA/5-HT levels under acute stress. I used the FST as an acute stressor, and collected samples just after the FST (Figure 3.8E). I observed that, in the NES model group, the 5-HIAA levels at ZT 13 and 5-HIAA/5-HT levels at ZT 1 were decreased (Figures 3.8F and 3.8H). To analyze the net effect of the acute stress on the 5-HT system, ratios of these parameters after FST treatment to those without FST treatment (after FST/no FST) were estimated. The NES model group showed that, compared with the control group, the 5-HIAA after FST/no FST at ZT 13, and 5-HT after FST/no FST at ZT 1 were decreased and increased, respectively. The 5-HIAA/5-HT after FST/no FST was lower than 1. These results might indicate that acute stress causes a decrease in the 5-HT metabolic rates. Moreover, the 5-HIAA/5-HT after FST/no FST in the NES model group at ZT 1 was significantly lower than that in the control group, suggesting that the FST would have a

stronger stress effect on the NES model group than on the control group (Figure 3.6I-3.6K).

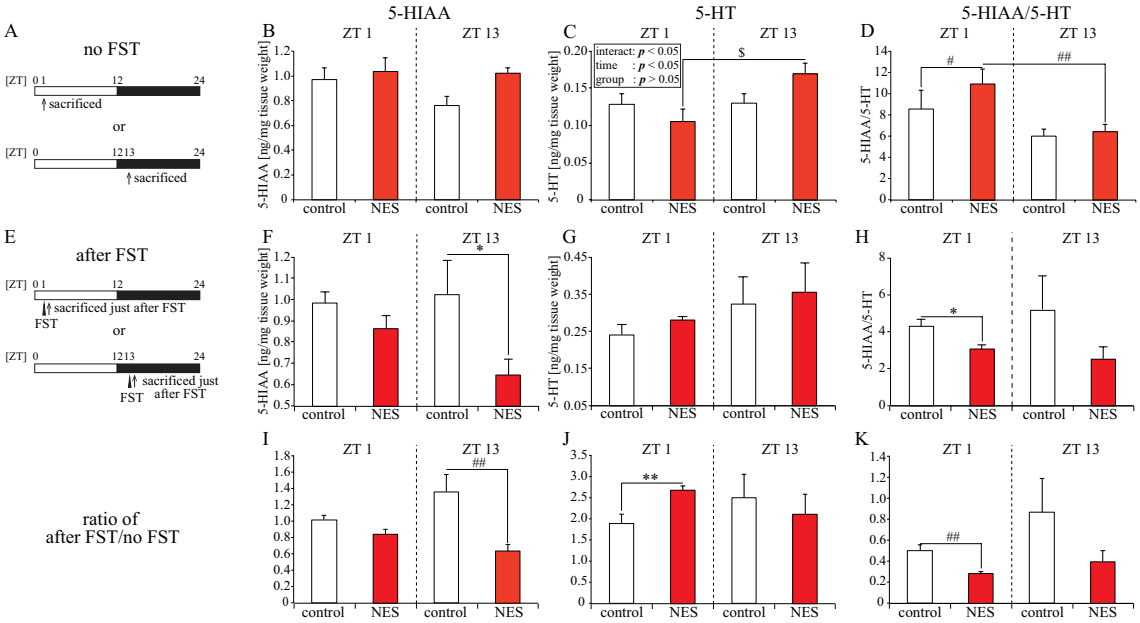

Figure 3.8 Effects of 5-minute RF with a HFD at ZT 5 and FF with a ND on 5-HT secretion and metabolism at ZT 1 and 13 with and without FST (Experiment 3.7)

(A) Sampling schedules. Mice were sacrificed at ZT 1 or 13 without FST after each feeding treatment for 4 weeks (no FST). Open and closed bars indicate the resting and active phases, respectively. (B-D) Levels of 5-HIAA (B) and 5-HT (C), and metabolic rates (5-HIAA/5-HT; D) in the hippocampus at ZT 1 or 13. (E) Sampling schedules. Mice were sacrificed at ZT 1 or 13 just after the FST after each feeding treatment for 4 weeks (after FST). (F-H) Levels of 5-HIAA (F) and 5-HT (G), and metabolic rates (H) in the hippocampus at ZT 1 and 13 just after the FST. (I-K) Stress reactivities of 5-HIAA (I), 5-HT (J), and metabolic rates (K) in the hippocampus. Levels were estimated by dividing each level after FST treatment by the average of the no FST treatment. Data are presented as the mean ± SEM (n = 6-8). * $p < 0.05$, ** $p < 0.01$ (Student *t*-test). # $p < 0.05$, ## $p < 0.01$ (Mann-Whitney test). $ $p < 0.05$ (two-way ANOVA with Tukey multiple comparison test). Results of two-way ANOVA of the data in 3.5B are shown.

3.3.8 Five-minute RF with a HFD and FF with a ND affected NE levels and NE metabolism in the hippocampus (Experiment 3.7)

To clarify the cause of time-specific depressive-like behavior in the NES model group, I measured the NE levels and ratio of MHPG/NE (metabolic rate) in the hippocampus. I observed that the NE, MHPG, and MHPG/NE levels in both groups under no FST treatment were similar at both measurement points (Figures 3.9A-3.9D). In after FST treatment, the NE and MHPG levels in the NES model group were increased and decreased, respectively, compared with those in the control group only at ZT 1 (Figures 3.9E-3.9G), and the MHPG/NE levels were also decreased in the NES model group at ZT 1 (Figure 3.9H). To analyze the net effect of acute stress on the NE system, I estimated ratios of NE and NE metabolite levels after FST treatment to those with no FST treatment (after FST/no FST). Interestingly, these ratios were greater than 1, indicating that acute stress causes the NE system activity. Changes in the NE, MHPG, and MHPG/NE (Figures 3.9I-3.9K) were similar to those occurring in groups after exposure to the FST (Figures 3.9F-3.9H).

In the NES model group, the FST as a stressor at ZT 1 caused an increase in 5-HT and NE secretion, but the FST decreased the utilization of monoamines and their metabolism compared with the control group. Taken together, these results suggest that a disrupted feeding rhythms leads to malfunction of stress reactivities of the 5-HT and NE systems at ZT 1, which may lead to time-specific depressive-like behavior.

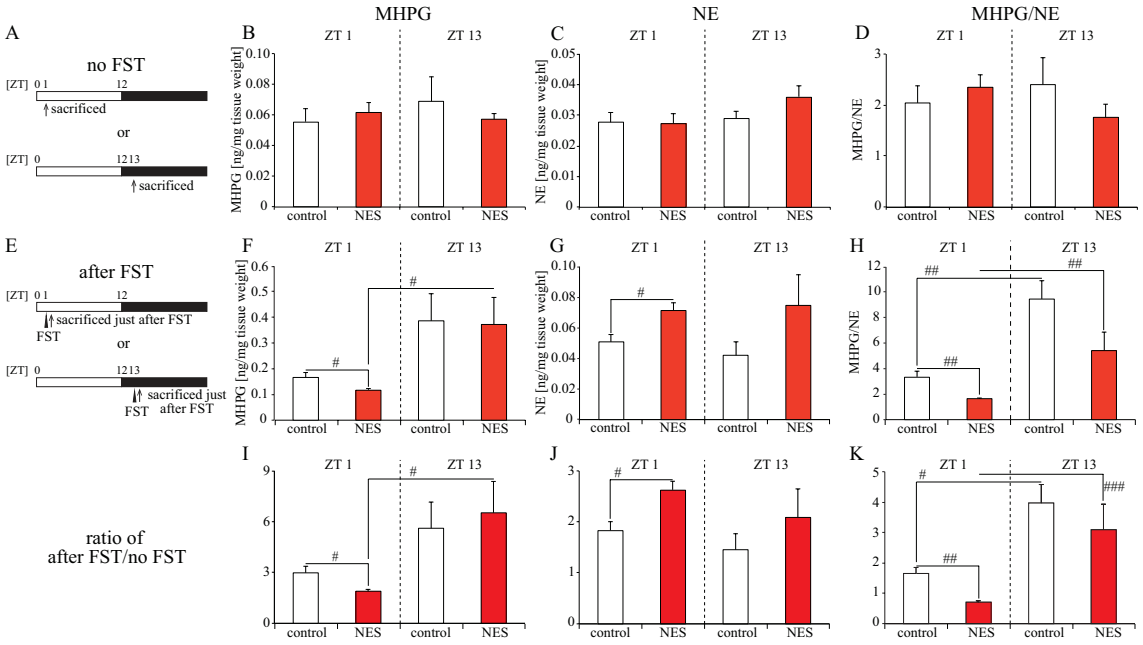

Figure 3.9 Effects of 5-minute RF with a HFD at ZT 5 and FF with a ND on NE secretion and metabolism at ZT 1 and 13 with and without FST (Experiment 3.7)

(A) Sampling schedules. Mice were sacrificed at ZT 1 or 13 without FST after each feeding treatment for 4 weeks (no FST). Open and closed bars indicate the resting and active phases, respectively. (B-D) Levels of MHPG (B), NE (C), and metabolic rates (MHPG/NE; D) in the hippocampus at ZT 1 and 13 after each feeding treatment for 4 weeks. (E) Sampling schedules. Mice were sacrificed at ZT 1 or 13 just after the FST after each feeding treatment for 4 weeks (after FST). (F-H) Levels of MHPG (F), NE (G), and metabolic rates (H) in the hippocampus at ZT 1 and 13 just after the FST. (I-K) Stress reactivities of MHPG (I), NE (J), and metabolic rates (K) in the hippocampus. Levels were estimated by dividing each level after FST treatment by the average of no FST treatment. Data are presented as the mean ± SEM (n = 6-8). # $p < 0.05$, ## $p < 0.01$, ### $p < 0.001$ (Mann-Whitney test).

3.3.9 Desipramine might decrease immobility time at ZT 1 induced by NES feeding patterns (Experiment 3.8)

To analyze whether the prolonged immobility time induced by the NES feeding treatment could be suppressed by desipramine (10 mg/kg), I conducted the FST 30 minutes after injection of mice with desipramine or saline. Desipramine is a tricyclic antidepressant that has been reported to show antidepressant-like effects on mice subjected to the FST (Yamada & Sugimoto, 2002; Shimazu et al., 2005). I found that immobility times in the NES-desipramine group tended to be shorter than in the NES-saline group, but there was no statistically significant difference (Figure 3.10). These results indicate that the time-specific depressive-like behavior induced by the NES feeding patterns may be improved by antidepressants, such as the tricyclic.

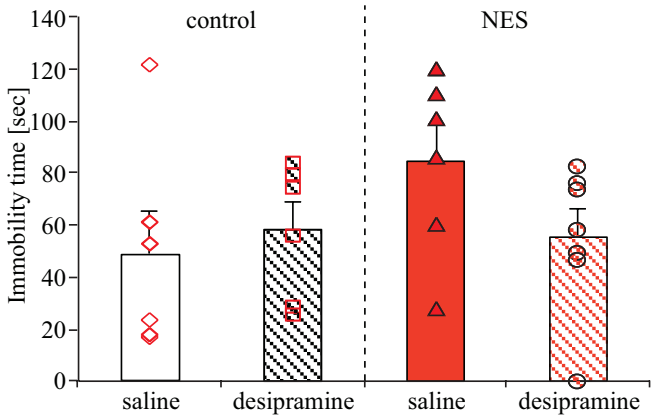

Figure 3.10 Effects of desipramine on immobility time in NES model mice induced by the NES feeding treatment (Experiment 3.8)

Immobility times at ZT 1 after maintaining mice under each feeding treatment for 4 weeks. Each symbol represents individual data. Mice under each feeding treatment were injected with saline or desipramine 30 minutes before the FST. Data are presented as the mean ± SEM (n = 6-7).

3.4 Discussion

In this chapter, I clarified the association between disrupted feeding rhythm and time-specific depressive-like behavior for the first time using a new NES model. First, I made a new NES mouse model, which imitated the eating patterns of patients with NES. Second, I demonstrated that the time-specific depressive-like behavior is caused by a disrupted feeding rhythm. Third, I suggested that the amount of calorie intake during the RF is an important factor of the time-specific depressive-like behavior. Fourth, I demonstrated that alteration in stress reactivity of the 5-HT and NE system (after FST/no FST), which is induced by a disrupted feeding rhythm, might be a cause of the time-specific depressive-like behavior. Last, I demonstrated that desipramine improves the time-specific depressive-like behavior of some mice in the NES model group. Taken together, the results of this chapter indicate that the development of time-specific depression is induced by a disrupted eating rhythm, and suggests that this NES model is a good model for elucidating the characteristics of patients with NES.

I established a NES model and demonstrated its reproducibility and validity. Under 5-minute RF with a HFD and FF with a ND, the NES model group received approximately 25% of its total calorie intake during RF, and total calorie intake was similar to that in the control group. Previous studies indicated that patients with NES got more calories during the night (resting phase) than during the day (active phase), and that their calorie intake per day was actually similar to that of healthy participants (Gluck et al., 2001). Moreover, one of the main criteria for NES is the consumption of at least 25% of the total daily calories after dinner (Allison et al., 2010). Relative locomotor activity levels in the NES model group were higher during the middle of the resting phase than in the control group. Moreover, their low relative

locomotor activity period was short and intermittent. Patients with NES experience frequent nocturnal awakening and have difficulty in maintaining sleep (Winkelman, 1998). The NES model group showed depressive-like behavior only at ZT 1. The mood of patients with NES were found to decline during the evening and night, contrary to the typical pattern of depression (Birketvedt et al., 1999). In previous studies, *Clock* mutant mice, EP3R or H1 receptor knockout mice, and RF of monkeys during the resting phase were defined as NES model animals (Masaki et al., 2004; Sullivan et al., 2005; Turek et al., 2005; Sanchez-Alavez et al., 2007). However, I judged that these mice or the feeding treatment would not be appropriate for analyzing the effects of disrupted feeding rhythms on time-specific depressive-like behavior. The reasons were that gene mutations, gene knock-out, and forced fasting themselves might have the potential to enhance or inhibit the depressive-like behavior (Li et al., 2015; Li et al., 2014). Recently, one study demonstrated that circulating ovarian hormones prevented a dysregulation of circadian rhythm and body weight gain induced by FF with a HFD treatment (Palmisano et al., 2017). In brief, body weights and circadian clock systems in the NES model group were likely to be affected by the disrupted feeding rhythm, and not by feeding with a HFD itself. Taken together, these results suggest that the new NES model, which was established based on the eating patterns of patients with NES, has high validity as a model.

I observed that immobility time was prolonged only at ZT 1 after 5-minute RF with a HFD and FF with a ND for 4 weeks, and I defined prolonged immobility time only at ZT 1 as time-specific depressive-like behavior. Previous studies showed that FF with a HFD for more than 20 weeks prolonged immobility time in the FST (Aslani et al., 2015), and that the Flinders Sensitive Line rat, a genetic model of depression, prolonged immobility time in the FST after

FF with a HFD for 8 weeks (Abildgaard, 2011). These results suggested that feeding rhythm is a more important factor in leading to depressive-like behavior than dietary components.

I furthermore demonstrated that the amount of calorie intake during 5-minute RF, which may have an effect in shifting peripheral clocks, might be an important factor in causing time-specific depressive-like behavior. Previous studies in mice indicated that RF during the resting phase shifts the peripheral clock, but not the central clock (Hara et al., 2001; Hirao et al., 2010; Kuroda et al., 2012), and a study in humans showed that delayed meals affected the adipose peripheral clock (Wehrens et al., 2017). Similar to these results, the results in this chapter showed that the NES feeding patterns advanced the phase of peripheral clocks only in the NES-5min (NES model) group (Figure 3.7). Stress factors, which had the potential to cause the depressive-like behavior, disrupted the association between the central and peripheral clocks (Cagampang et al., 2011). Accordingly, disruption of the association between the central and peripheral clocks may lead to depressive-like behavior. Moreover, a study in humans suggested that misalignment of social and biological clocks would increase the risk of developing of depression (Levandovski et al., 2011). Other studies in humans showed that abnormal circadian rhythms are observed in seasonal affective disorder, bipolar disorder, and other mood disorders (Goodwin & Jamison, 2007; Levitan, 2007; Lewy, 2007). A study in mice demonstrated that an abnormal LD cycle caused mice arrhythmicity, damped clock gene expression rhythms in the hippocampus, and prolonged immobility times (Moriya et al., 2015). I measured clock gene expression rhythms in peripheral clocks *in vivo*, and observed an advanced phase of peripheral clocks in only the NES-5min (NES model) group. Previous studies suggested that decreased sleep quality would cause depression symptoms (Ford & Kamerow, 1989; Perlis et al., 1997). In

the NES-2min group, relative locomotor activity levels during the middle of the resting phase were higher than those in the control group, but their immobility times at ZT 1 were similar to those in the control group. Moreover, immobility times in the NES-ZT5-ND group were similar to those in the control group, although sleep in the NES-ZT5-ND group was disrupted by RF with a ND. Furthermore, immobility times in the NES-ZT17-HFD group were similar to that in the control group, although they ate a HFD. Accordingly, the time-specific depressive-like behavior in the NES model group is thought to be caused by a disrupted feeding rhythm, and not by repeated sleep disturbance and feeding with a HFD. Taken together, these results indicate that the disrupted feeding rhythm would shift the phase of peripheral clocks, and then these shifts may cause time-specific depressive-like behavior.

I demonstrated that disrupted feeding rhythms caused depressive-like behavior only at ZT 1, which would correspond to the evening and early night for humans. Our previous study indicated that subacute physical stress around ZT 1 caused internal desynchronization in the circadian clocks of peripheral tissues (Tahara et al., 2015). In brief, physical stress around ZT 1 might induce abnormal reactions at least in the circadian clock system. Previous studies indicated that the FST increased and/or decreased the levels of 5-HT, 5-HIAA, NE, and MHPG, as well as their metabolic rates. However, results differed among the studies (Miura et al., 1993; Jordan et al., 1994; Abercrombie et al., 1988; Nakazawa et al., 2003). In this chapter, the ratios of after FST/no FST in the metabolic rates of both monoamines (5-HT and NE) in the NES model group were lower than those in the control group at ZT 1, although the ratios of after FST/no FST in both monoamines in the NES model group were higher. In brief, compared with the control group, the synthesis of 5-HT and NE in the NES model group was activated by acute

stress (FST) at ZT 1, but the utilization and metabolism of these monoamines might not be adequately activated. These results imply that a disrupted feeding rhythm would cause time-specific depressive-like behavior, and from a monoamine metabolism perspective, would induce and/or disuse of the 5-HT and NE under acute stress rather than the synthesis of these monoamines.

In this chapter, I suggest that phase shifts of peripheral clocks and malfunction and/or disuse of the 5-HT and NE in the hippocampus is the cause of the time-specific depressive-like behavior. I was unable to measure the PER2::LUC bioluminescence rhythm in the hippocampus because of technical reasons. However, I hypothesized that the PER2::LUC bioluminescence rhythm in the hippocampus may be shifted by the NES feeding patterns, because a previous study showed that RF during the resting phase shifted the phase of the PER2::LUC bioluminescence rhythm in the hippocampus (Loh et al., 2015). Moreover, Tahara et al. (2011) indicated that RF caused a phase shift of not only *Per2* expression rhythm but also the expression rhythms of other clock genes in the liver. A recent study suggested that changes in the expression of clock genes would cause depression symptoms (Calabrese et al., 2016). The expression rhythms of *Maoa* and *catechol-O-methyltransferase* (*Comt*), which are genes encoding degradation enzymes of monoamine, are controlled by clock genes and glucocorticoid (Albrecht, 2017). Taken together, these reports suggest that the NES feeding patterns would shift the phase of clock gene expression rhythms in the hippocampus, which would subsequently change *Maoa* and *Comt* expression rhythms, leading to malfunction and/or disuse of the 5-HT and NE in the hippocampus.

I also found that desipramine prevented prolonged immobility time of some mice in

the NES-desipramine group compared with mice in the NES-saline group. In fact, previous studies showed that the administration of some drugs, such as topiramate and escitalopram, resulted in the recovery from depression symptoms of half the patients with NES (O'Reardon et al., 2004; Allison et al., 2013). However, It is unclear as to why the effects of desipramine on time-specific depressive-like behavior have individual differences.

In this chapter, I made a new NES model based on the eating patterns of patients with NES, and demonstrated the association between a disrupted feeding rhythm and time-specific depressive-like behavior for the first time. Furthermore, my results suggested that the disrupted feeding rhythm would cause malfunction of the 5-HT and NE under acute stress, leading to time-specific depressive-like behavior. Moreover, the amount of calorie intake during 5-minute RF is an important factor associated with time-specific depressive-like behavior (Figure 3.11). I expect that these results will be of wide interest to the public, because many people nowadays play or work during the night, such as shift workers and nurses, and some people eat food during the night. Furthermore, I believe that using this NES mouse model may help to establish a new therapy for patients with NES, and also clarify the characteristics of patients with NES. These reasons are that almost all of research on NES had only been performed using human subjects, and that studies of NES have been still preliminary (Kucukgoncu et al., 2015).

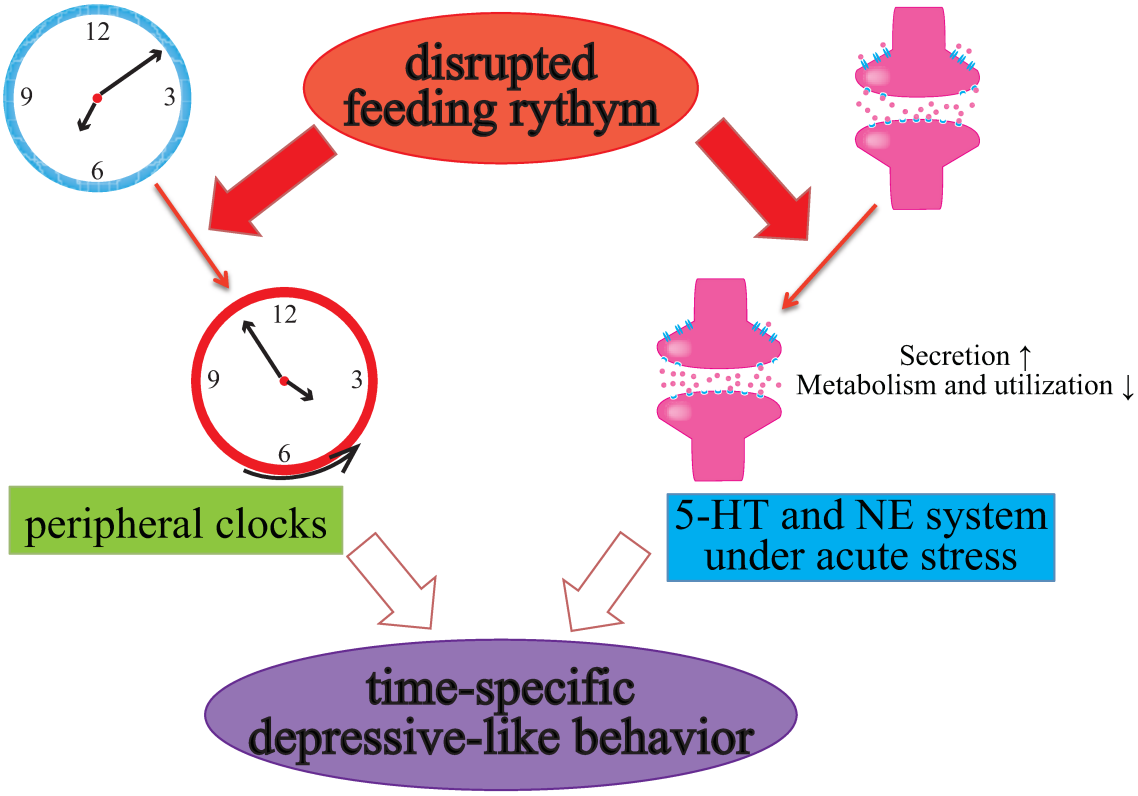

Figure 3.11 Working model of the effects of the disrupted feeding rhythm on peripheral clocks and 5-HT and NE systems in the hippocampus

A disrupted feeding rhythm would advance the shift of peripheral clocks and would cause malfunction of the 5-HT and NE systems under stress, leading to time-specific depressive-like behavior.

Chapter 4. Conclusion and future prospects

In modern society, many healthy adults change their eating patterns every day and consume foods during a period of 15 hours or longer of each day, meaning from the first meal after waking up to the last meal before going to bed (Gill & Panda, 2015). In chapter 2, I demonstrated that meals during the resting phase would increase the risks of an increase in body weight, accumulation of visceral fat, and shift of the circadian rhythm in the liver. In chapter 3, I demonstrated the association between disrupted feeding rhythm and time-specific depressive-like behavior. Taken together, the results in this thesis suggest that not only food composition, but meal pattern based on circadian rhythm is an important factor for maintaining human health in modern society.

In the future, I would like to conduct a study on chrono-nutrition. For example, caffeine and nobiletin prolong the circadian period and increase the amplitude of circadian oscillation, respectively, and both were found to have anti-obesity effects (Oike et al., 2011; Burke et al., 2015; Narishige et al., 2014; He et al., 2016; Lopez-Garcia et al., 2006). However, the chrono-nutritional effects of both of these reagents have not yet been investigated. RF itself has anti-obesity effects (Hatori et al., 2012; Sherman et al., 2012), and RF with too short a duration might cause obesity, as shown in chapter 2. In chapter 2, I also demonstrated that body weights and amount of visceral fat in the 8-8[HFD-ND] group were increased compared with those in the 8-8[ND-HFD] group. Accordingly, I would like to analyze the time-dependent effects of nutrition, such as foods with function claims, caffeine, nobiletin, and other nutrition on obesity using 8-hour RF treatment. For example, it will be interesting to investigate which RF with a HFD containing caffeine during the resting phase or during the active phase,

mimicking human dinner and breakfast, respectively, has anti-obesity effects, using 8-hour RF treatment.

Depression is known to affect about 3%-10% of the general population (World Health Organization, 2013). In chapter 3, I identified a new cause of depression symptoms. In brief, my results suggested the importance for people to maintain an adequate eating rhythm, particularly shift workers and nurses. I also demonstrated the mechanism of how disrupted feeding rhythms induce time-specific depressive-like behavior using this NES model for research on therapeutics for NES. Previous studies have developed a new and noninvasive method to measure human circadian clock gene rhythms using hair follicle cells (Akashi et al., 2010; Watanabe et al., 2012), and this method is available in our laboratory (Takahashi et al., 2017). Therefore, in the future I would like to monitor human circadian clock gene expression rhythms in patients with NES before and after treatment. Moreover, I would like to clarify the association among time-specific depression symptoms, amount of calories consumed between dinner and bedtime, and the expression rhythms of human circadian clock genes.

Acknowledgements

First of all, I would like to express my appreciation and gratitude to my supervisor, **Professor Shigenobu Shibata**, for supporting me in my doctoral project, giving me many good experiences, including participation three international conferences.

I would also like to appreciate the referees of my doctor thesis, **Professor Toshiyuki Okano** and **Professor Toru Asahi** in Waseda University, and **Dr. Keiji Kondo** in Kirin Company, Ltd., for their helpful feedback and constant encouragement during my doctoral project.

I would also like to express my gratitude to **Professor Christopher S. Colwell** in the University of California, Los Angeles (UCLA) for giving me a chance to perform research in UCLA for three months and giving me valuable feedback on my doctoral studies.

I would like to deeply thank **Dr. Yu Tahara**, **Dr. Akiko Furutani**, and **Dr. Natsumi Aoki,** who have been my superiors from 2011 when I started to work in the Shibata lab. They always gave me warm and encouraging comments, technical advice, and helpful discussions.

I am greatly indebted to **Mr. Takafumi Fukuda** in Kirin Company, Ltd., for collaborating with me from 2013 and supporting my internship program in Kirin Company, Ltd., for three months.

I am grateful to all members and staff of the Shibata lab. I would like to mention a special thanks to **Ms. Miyabi Fukuzawa** and **Mr. Yutaro Nishimura** for helping me with my experiments.

I would like to thank **Ms. Yuko Ikeda**; we have worked hard together and helped each other from 2011.

Lastly, I would like to express my deep appreciation to my family, **Hiroshi**, **Masayo**, and **Rie**, for always supporting me unconditionally.

A.H. was supported by a Grant-in-Aid for Japan Society for the Promotion of Science (JSPS) Research Fellow (17J10069), and the Leading Graduate Program of Science and Engineering, Waseda University from MEXT.

References

Abercrombie, E. D., Keller, R. W. Jr. & Zigmond, M. J. Characterization of hippocampal norepinephrine release as measured by microdialysis perfusion: pharmacological and behavioral studies. Neuroscience. 27, 897-904 (1988).

Abildgaard, A. A high-fat diet exacerbates depressive-like behavior in the Flinders Sensitive Line (FSL) rat, a genetic model of depression. Psychoneuroendocrinology. 36, 623-633 (2011).

Akashi, M., Soma, H., Yamamoto, T., Tsugitomi, A., Yamashita, S., Yamamoto, T., Nishida, E., Yasuda, A., Liao, J. K. & Node, K. Noninvasive method for assessing the human circadian clock using hair follicle cells. Proc Natl Acad Sci U S A. 107, 15643-15648 (2010).

Albrecht, U. Molecular Mechanisms in Mood Regulation Involving the Circadian Clock. Front Neurol. 8, 30 (2017).

Albrecht, U. Timing to perfection: the biology of central and peripheral circadian clocks. Neuron. 74, 246-260 (2012).

Allison, K. C., Lundgren, J. D., O'Reardon, J. P., Geliebter, A., Gluck, M. E., Vinai, P., Mitchell, J. E., Schenck, C. H., Howell, M. J., Crow, S. J., Engel, S., Latzer, Y., Tzischinsky, O., Mahowald, M. W. & Stunkard, A. J. Proposed diagnostic criteria for night eating syndrome. Int

J Eat Disord. 43, 241-247 (2010).

Allison, K. C., Studt, S. K., Berkowitz, R. I., Hesson, L. A., Moore, R. H., Dubroff, J. G., Newberg, A. & Stunkard, A. J. An open-label efficacy trial of escitalopram for night eating syndrome. Eat Behav. 14, 199-203 (2013).

Allison, K. C. & Stunkard, A. J. Obesity and eating disorders. Psychiatr Clin North Am. 28, 55-67 (2005).

Anderson, I. M., Nutt, D. J. & Deakin, J. F. W. Evidence-based guidelines for treating depressive disorders with antidepressants: a revision of the 1993 British Association for Psychopharmacology guidelines. J Psychopharmacol. 4, 3-20 (2000).

Andrews, J. L., Zhang, X., McCarthy, J. J., McDearmon, E. L., Hornberger, T. A., Russell, B., Campbell, K. S., Arbogast, S., Reid, M. B., Walker, J. R., Hogenesch, J. B., Takahashi, J. S. & Esser, K. A. CLOCK and BMAL1 regulate MyoD and are necessary for maintenance of skeletal muscle phenotype and function. Proc Natl Acad Sci U S A. 107, 19090-19095 (2010).

Aoyama, S. & Shibata, S. The Role of Circadian Rhythms in Muscular and Osseous Physiology and Their Regulation by Nutrition and Exercise. Front Neurosci. 11, 63 (2017).

Arble, D. M., Bass, J., Laposky, A. D., Vitaterna, M. H. & Turek, F. W. Circadian timing of

food intake contributes to weight gain. Obesity (Silver Spring). 17, 2100-2102 (2009).

Asher, G. & Schibler, U. Crosstalk between components of circadian and metabolic cycles in mammals. Cell Metab. 13, 125-137 (2011).

Aslani, S., Vieira, N., Marques, F., Costa, P. S., Sousa, N. & Palha, J. A. The effect of high-fat diet on rat's mood, feeding behavior and response to stress. Transl Psychiatry. 24, e684 (2015).

Bailey, S. M., Udoh, U. S. & Young, M. E. Circadian regulation of metabolism. J Endocrinol. 222, R75-R96 (2014).

Bass, J. & Takahashi, J. S. Circadian integration of metabolism and energetics. Science. 330, 1349-1354 (2010).

Birketvedt, G. S., Florholmen, J., Sundsfjord, J., Osterud, B., Dinges, D., Bilker, W. & Stunkard, A. Behavioral and neuroendocrine characteristics of the night-eating syndrome. JAMA. 282, 657-663 (1999).

Borsini, F., Lecci, A., Sessarego, A., Fressine, R. & Meli, A. Discovery of antidepressant activity by forced swimming test may depend on pre-exposure of rats to a stressful situation. Psychopharmacology (Berl). 97, 183-188 (1989).

Bray, M. S., Tsai, J. Y., Villegas-Montoya, C., Boland, B. B., Blasier, Z., Egbejimi, O., Kueht, M. & Young, M. E. Time-of-day-dependent dietary fat consumption influences multiple cardiometabolic syndrome parameters in mice. Int J Obes (Lond). 34, 1589-1598 (2010).

Brunello, N. Noradrenaline in mood and anxiety disorders: basic and clinical studies. Int Clin Psychopharmacol. 18, 191-202. (2003)

Buhr, E. D. & Takahashi, J. S. Molecular components of the mammalian circadian clock. Handb Exp Pharmacol. 217, 3-27 (2013).

Buijs, R. M., van Eden, C. G., Goncharuk, V. D. & Kalsbeek, A. The biological clock tunes the organs of the body: Timing by hormones and the autonomic nervous system. Rev J Endocrinol. 177, 17-26 (2003).

Burke, T. M., Markwald, R. R., McHill, A. W., Chinoy, E. D., Snider, J. A., Bessman, S. C., Jung, C. M., O'Neill, J. S. & Wright, K. P. Jr. Effects of caffeine on the human circadian clock in vivo and in vitro. Sci Transl Med. 7, 305ra146 (2015).

Cagampang, F. R., Poore, K. R. & Hanson, M. A. Developmental origins of the metabolic syndrome: body clocks and stress responses. Brain Behav Immun. 25, 214-220 (2011).

Calabrese, F., Savino, E., Papp, M., Molteni, R. & Riva, M. A. Chronic mild stress-induced

alterations of clock gene expression in rat prefrontal cortex: modulatory effects of prolonged lurasidone treatment. Pharmacol Res. 104, 140-150 (2016).

Delezie, J. & Challet, E. Interactions between metabolism and circadian clocks: reciprocal disturbances. Rev. Ann N Y Acad Sci. 1243, 30-46 (2011).

Filipski, E., Li, X. M. & Lévi, F. Disruption of circadian coordination and malignant growth. Cancer Causes Control. 17, 509-514 (2006).

Ford, D. E. & Kamerow, D. B. Epidemiologic study of sleep disturbances and psychiatric disorders. An opportunity for prevention? JAMA. 262, 1479-1484 (1989).

Froy, O. Circadian rhythms and obesity in mammals. Rev. ISRIN Obes. 2012, 437198 (2012).

Fukuda, T., Haraguchi, A., Kuwahara, M., Nakamura, K., Hamaguchi, Y., Ikeda, Y., Ishida, Y., Wang, G., Shirakawa, C., Tanihata, Y., Ohara, K. & Shibata, S. l-Ornithine affects peripheral clock gene expression in mice. Sci Rep. 6, 34665 (2016).

Gachon, F., Nagoshi, E., Brown, S. A., Ripperger, J. & Schibler, U. The mammalian circadian timing system: from gene expression to physiology. Chromosoma. 113, 103-112 (2004).

Garaulet, M. & Madrid, J. A. Chronobiological aspects of nutrition, metabolic syndrome and

obesity. Rev. Adv Drug Deliv. 62, 967-978 (2010).

Gill, S. & Panda, S. A Smartphone App Reveals Erratic Diurnal Eating Patterns in Humans that Can Be Modulated for Health Benefits. Cell Metab. 22, 789-798 (2015).

Gluck, M. E., Geliebter, A. & Satov, T. Night eating syndrome is associated with depression, low self-esteem, reduced daytime hunger, and less weight loss in obese outpatients. Obes Res. 9, 264-267 (2001).

Golombek, D. A. & Rosenstein, R. E. Physiology of circadian entrainment. Physiol. Rev. 90, 1063-1102 (2010).

Goodwin, F. K. & Jamison, K. R. Bipolar Disorders and Recurrent Depression. Manic-depressive illness. 2nd edition. New York, NY 659-698 (Oxford University Press, 2007).

Gooley, J. J. Circadian regulation of lipid metabolism. Proc Nutr Soc. 75, 440-450 (2016).

Hampp, G., Ripperger, J. A., Houben, T., Schmutz, I., Blex, C., Perreau-Lenz, S., Brunk, I., Spanagel, R., Ahnert-Hilger, G., Meijer, J. H. & Albrecht, U. Regulation of monoamine oxidase A by circadian-clock components implies clock influence on mood. Curr Biol. 18, 678-683 (2008).

Hara, R., Wan, K., Wakamatsu, H., Aida, R., Moriya, T., Akiyama, M. & Shibata, S. Restricted feeding entrains liver clock without participation of the suprachiasmatic nucleus. Genes Cells. 6, 269-278 (2001).

Haraguchi, A., Aoki, N., Ohtsu, T., Ikeda, Y., Tahara, Y. & Shibata, S. Controlling access time to a high-fat diet during the inactive period protects against obesity in mice. Chronobiol Int. 31, 935-944 (2014).

Hastings, M. H. Central clocking. Rev Trends Neurosci. 20, 459-464 (1997).

Hatori, M., Vollmers, C., Zarrinpar, A., DiTacchio, L., Bushong, E. A., Gill, S., Leblanc, M., Chaix, A., Joens, M., Fitzpatrick, J. A., Ellisman, M. H. & Panda, S. Time-Restricted Feeding without Reducing Caloric Intake Prevents Metabolic Diseases in Mice Fed a High fat Diet. Cell Metab. 15, 848-860 (2012).

He, B., Nohara, K., Park, N., Park, Y. S., Guillory, B., Zhao, Z., Garcia, J. M., Koike, N., Lee, C. C., Takahashi, J. S., Yoo, S. H. & Chen, Z. The Small Molecule Nobiletin Targets the Molecular Oscillator to Enhance Circadian Rhythms and Protect against Metabolic Syndrome. Cell Metab 23, 610-621 (2016).

He, Q., Ding, Z. Y., Fong, D. Y. & Karlberg, J. Risk factors of obesity in preschool children in China: a population-based case--control study. Int J Obes Relat Metab Disord. 24, 1528-1536

(2000).

Hirao, A., Nagahama, H., Tsuboi, T., Hirao, M., Tahara, Y. & Shibata, S. Combination of starvation interval and food volume determines the phase of liver circadian rhythm in Per2::Luc knock-in mice under two meals per day feeding. Am J Physiol Gastrointest Liver Physiol. 299, G1045-G1053 (2010).

Hughes, M. E., DiTacchio, L., Hayes, K. R., Vollmers, C., Pulivarthy, S., Baggs, J. E., Panda, S. & Hogenesch, J. B. Harmonics of circadian gene transcription in mammals. PLoS Genet. 5, e1000442 (2009).

Inoue, Y. Sleep-related eating disorder and its associated conditions. Psychiatry Clin Neurosci. 69, 309-320 (2015).

Jordan, S., Kramer, G. L., Zukas, P. K. & Petty, F. Previous stress increases in vivo biogenic amine response to swim stress. Neurochem Res. 19, 1521-1525 (1994).

Kageyama, A., Sakakibara, H., Zhou, W., Yoshioka, M., Ohsumi, M., Shimoi, K. & Yokogoshi, H. Genistein regulated serotonergic activity in the hippocampus of ovariectomized rats under forced swimming stress. Biosci Biotechnol Biochem. 74, 2005-2010 (2010).

Kalsbeek, A., Fliers, E., Romijn, J. A., La Fleur, S. E., Wortel, J., Bakker, O., Endert, E. &

Buijs, R. M. The suprachiasmatic nucleus generates the diurnal changes in plasma leptin levels. Endocrinology. 142, 2677-2685 (2001).

Karatsoreos, I. N., Bhagat, S., Bloss, E. B., Morrison, J. H. & McEwen, B. S. Disruption of circadian clocks has ramifications for metabolism, brain, and behavior. Proc Natl Acad Sci U S A. 108, 1657-1662 (2011).

Kennedy, S. H., Lam, R. W., Cohen, N. L. & Ravindran, A. V. CANMAT Depression Work Group. Clinical guidelines for the treatment of depressive disorders. IV. Medications and other biological treatments. Can J Psychiatry. 46, 38S-58S (2001).

Kirsz, K. & Zieba, D. A. A review on the effect of the photoperiod and melatonin on interactions between ghrelin and serotonin. Gen Comp Endocrinol. 179, 248-253 (2012).

Kohsaka, A., Laposky, A. D., Ramsey, K. M., Estrada, C., Joshu, C., Kobayashi, Y., Turek, F. W. & Bass, J. High fat diet disrupts behavioral and molecular circadian rhythms in mice. Cell Metab. 6, 414-421 (2007).

Kucukgoncu, S., Midura, M. & Tek, C. Optimal management of night eating syndrome: challenges and solutions. Neuropsychiatr Dis Treat. 11, 751-760 (2015).

Kuroda, H., Tahara, Y., Saito, K., Ohnishi, N., Kubo, Y., Seo, Y., Otsuka, M., Fuse, Y., Ohura,

Y., Hirao, A. & Shibata S. Meal frequency patterns determine the phase of mouse peripheral circadian clocks. Sci Rep. 2, 711 (2012).

Lamia, K. A., Storch, K. F. & Weitz, C. J. Physiological significance of a peripheral tissue circadian clock. Proc Natl Acad Sci U S A. 105, 15172-15177 (2008).

Levandovski, R., Dantas, G., Fernandes, L. C., Caumo, W., Torres, I., Roenneberg, T., Hidalgo, M. P. & Allebrandt, K. V. Depression scores associate with chronotype and social jetlag in a rural population. Chronobiol Int. 28, 771-778 (2011).

Levitan, R. D. The chronobiology and neurobiology of winter seasonal affective disorder. Dialogues Clin Neurosci. 9, 315-324 (2007).

Lewy, A. J. Depressive disorders may more commonly be related to circadian phase delays rather than advances: time will tell. Sleep Med. 11, 117-118 (2010).

Lewy, A. J. The phase shift hypothesis for the circadian component of winter depression. Dialogues Clin Neurosci. 9, 291-300 (2007).

Li, B., Zhao, J., Lv, J., Tang, F., Liu, L., Sun, Z., Wang, L., Siwela, S. P., Wang, Y., Song, Y., Manchishi, S. M. & Cui, R. Additive antidepressant-like effects of fasting with imipramine via modulation of 5-HT2 receptors in the mice. Prog Neuropsychopharmacol Biol Psychiatry. 48,

199-206 (2014).

Li, N., Xu, Y., Chen, X., Duan, Q. & Zhao, M. Sex-specific diurnal immobility induced by forced swim test in wild type and clock gene deficient mice. Int J Mol Sci. 16, 6831-6841 (2015).

Li, S., Wang, C., Li, W., Koike, K., Nikaido, T. & Wang, M. W. Antidepressant-like effects of piperine and its derivative, antiepilepsirine. J Asian Nat Prod Res. 9, 421-430 (2007).

Lin, S. H., Chen, W. C., Lu, K. H., Chen, P. J., Hsieh, S. C., Pan, T. M., Chen, S. T. & Sheen, L. Y. Down-regulation of Slit-Robo pathway mediating neuronal cytoskeletal remodeling processes facilitates the antidepressive-like activity of Gastrodia elata Blume. J. Agricult. Food Chem. 62, 10493-10503 (2014).

Loh, D. H., Jami, S. A., Flores, R. E., Truong, D., Ghiani, C. A., O'Dell, T. J. & Colwell, C. S. Misaligned feeding impairs memories. Elife. 4, pii: e09460 (2015).

Lopez-Garcia, E., van Dam, R. M., Rajpathak, S., Willett, W. C., Manson, J. E. & Hu, F. B. Changes in caffeine intake and long-term weight change in men and women. Am. J. Clin. Nutr. 83, 674-680 (2006).

Martínez-González, M. A. & Sánchez-Villegas, A. Food patterns and the prevention of

depression. Proc Nutr Soc. 75, 139-146 (2016).

Masaki, T., Chiba, S., Yasuda, T., Noguchi, H., Kakuma, T., Watanabe, T., Sakata, T. & Yoshimatsu, H. Involvement of hypothalamic histamine H1 receptor in the regulation of feeding rhythm and obesity. Diabetes. 53, 2250-2260 (2004).

Matsuno, K., Kobayashi, T., Tanaka, M. K. & Mita, S. Sigma 1 receptor subtype is involved in the relief of behavioral despair in the mouse forced swimming test. Eur J Pharmacol. 312, 267-271 (1996).

Mi, Y., Qi, G., Fan, R., Ji, X., Liu, Z. & Liu, X. EGCG ameliorates diet-induced metabolic syndrome associating with the circadian clock. Biochim Biophys Acta. 1863, 1575-1589 (2017).

Miller, B. H., McDearmon, E. L., Panda, S., Hayes, K. R., Zhang, J., Andrews, J. L., Antoch, M. P., Walker, J. R., Esser, K. A., Hogenesch, J. B. & Takahashi, J. S. Circadian and CLOCK-controlled regulation of the mouse transcriptome and cell proliferation. Proc Natl Acad Sci U S A. 104, 3342-3347 (2007).

Mistlberger, R. E. Neurobiology of food anticipatory circadian rhythms. Rev. Physiol Behav. 104, 535-545 (2011).

Miura, H., Naoi, M., Nakahara, D., Ohta, T. & Nagatsu, T. Changes in monoamine levels in mouse brain elicited by forced-swimming stress, and the protective effect of a new monoamine oxidase inhibitor, RS-8359. J Neural Transm Gen Sect. 94, 175-187 (1993).

Mohawk, J. A., Green, C. B. & Takahashi, J. S. Central and peripheral circadian clocks in mammals. Annu Rev Neurosci. 35, 445-462 (2012).

Moriya, S., Tahara, Y., Sasaki, H., Ishigooka, J. & Shibata, S. Housing under abnormal light-dark cycles attenuates day/night expression rhythms of the clock genes Per1, Per2, and Bmal1 in the amygdala and hippocampus of mice. Neurosci Res. 99, 16-21 (2015).

Mouret, J., Coindet, J., Debilly, G. & Chouvet, G. Suprachiasmatic nuclei lesions in the rat: alterations in sleep circadian rhythms, Electroencephalogr Clin Neurophysiol 45, 402-408 (1978).

Mulrow, C. D., Williams, J. W. Jr., Trivedi, M., Chiquette, E., Aguilar, C., Cornell, J. E., Badgett, R., Noël, P. H., Lawrence, V., Lee, S., Luther, M., Ramirez, G., Richardson, W. S. & Stamm, K. Treatment of depression--newer pharmacotherapies. Psychopharmacol Bull. 34, 409-795 (1999).

Nakazawa, T., Yasuda, T., Ueda, J. & Ohsawa, K. Antidepressant-like effects of apigenin and 2,4,5-trimethoxycinnamic acid from Perilla frutescens in the forced swimming test. Biol Pharm

Bull. 26, 474-480 (2003).

Narishige, S., Kuwahara, M., Shinozaki, A., Okada, S., Ikeda, Y., Kamagata, M., Tahara, Y. & Shibata. S. Effects of caffeine on circadian phase, amplitude and period evaluated in cells in vitro and peripheral organs in vivo in PER2::LUCIFERASE mice. Br J Pharmacol. 171, 5858-5869 (2014).

Nechita, F., Pîrlog, M. C. & ChiriŢă, A. L. Circadian malfunctions in depression - neurobiological and psychosocial approaches. Rom J Morphol Embryol. 56, 949-955 (2015).

Nelson, R. & Zucker, I. Absence of extraocular photoreception in diurnal and nocturnal rodents exposed to direct sunlight. Comp Biochem Physiol. 69A, 145-148 (1981).

Ochiai, H., Shirasawa, T., Ohtsu, T., Nishimura, R., Morimoto, A., Hoshino, H., Tajima, N. & Kokaze, A. Eating behaviors and overweight among adolescents: A population-based survey in Japan. J Obes. 2013, 717942 (2013).

Oike, H., Kobori, M., Suzuki, T. & Ishida, N. Caffeine lengthens circadian rhythms in mice. Biochem Biophys Res Commun. 410, 654-658 (2011).

Oishi, K., Miyazaki, K., Kadota, K., Kikuno, R., Nagase, T., Atsumi, G., Ohkura, N., Azama, T., Mesaki, M., Yukimasa, S., Kobayashi, H., Iitaka, C., Umehara, T., Horikoshi, M., Kudo, T.,

Shimizu, Y., Yano, M., Monden, M., Machida, K., Matsuda, J., Horie, S., Todo, T. & Ishida, N. Genome-wide expression analysis of mouse liver reveals CLOCK-regulated circadian output genes. J. Biol. Chem. 278, 41519-41527 (2003).

O'Reardon, J. P., Stunkard, A. J. & Allison, K. C. Clinical trial of sertraline in the treatment of night eating syndrome. Int J Eat Disord. 35, 16-26 (2004).

Otsuka, R., Tamakoshi, K., Yatsuya, H., Murata, C., Sekiya, A., Wada, K., Zhang, H. M., Matsushita, K., Sugiura, K., Takefuji, S., OuYang, P., Nagasawa, N., Kondo, T., Sasaki, S. & Toyoshima, H. Eating fast leads to obesity: findings based on self-administered questionnares among middle-aged Japanese men and women. J Epidemiol. 16, 117-124 (2006).

Palmisano, B. T., Stafford, J. M. & Pendergast, J. S. High-Fat Feeding Does Not Disrupt Daily Rhythms in Female Mice because of Protection by Ovarian Hormones. Front Endocrinol (Lausanne). 8, 44 (2017).

Pendergast, J. S., Branecky, K. L., Yang, W., Ellacott, K. L., Niswender, K. D. & Yamazaki, S. High fat diet acutely affects circadian organization and eating behavior. Eur J Neurosci. 37, 1350-1356 (2013).

Perlis, M. L., Giles, D. E., Buysse, D. J., Tu, X. & Kupfer, D. J. Self-reported sleep disturbance as a prodromal symptom in recurrent depression. J Affect Disord. 42, 209-212 (1997).

Porsolt, R. D., Bertin, A., Blavet, N., Deniel, M. & Jalfre, M. Immobility induced by forced swimming in rats: effects of agents which modify central catecholamine and serotonin activity. Eur. J. Pharmacol. 57, 201-210 (1979).

Porsolt, R. D., Pichon, M. L. & Jalfre, M. Depression: a new animal model sensitive to antidepressant treatments. Nature. 266, 730-732 (1977).

Refinetti, R., Lissen, G. C. & Halberg, F. Procedures for numerical analysis of circadian rhythms. Biol Rhythm Res. 38, 275-325 (2007).

Salgado-Delgado, R., Angeles-Castellanos, M., Saderi, N., Buijs, R. M. & Escobar, C. Food intake during the normal activity phase prevents obesity and circadian desynchrony in a rat model of night work. Endocrinology. 151, 1019-1029 (2010).

Sanchez-Alavez, M., Klein, I., Brownell, S. E., Tabarean, I. V., Davis, C. N., Conti, B. & Bartfai, T. Night eating and obesity in the EP3R deficient mouse. Proc Natl Acad Sci U S A. 104, 3009-3014 (2007).

Sasaki, H., Hattori, Y., Ikeda, Y., Kamagata, M., Iwami, S., Yasuda, S. & Shibata, S. Phase shifts in circadian peripheral clocks caused by exercise are dependent on the feeding schedule in PER2::LUC mice. Chronobiol Int. 33, 849-862 (2016).

Sato, M., Nakamura, K., Ogata, H., Miyashita, A., Nagasaka, S., Omi, N., Yamaguchi, S., Hibi, M., Umeda, T., Nakaji, S. & Tokuyama, K. Acute effect of late evening meal on diurnal variation of blood glucose and energy metabolism. Obes Res Clin Pract. 5, e169-e266 (2011).

Schibler, U., Ripperger, J. & Brown, S. A. Peripheral circadian oscillators in mammals: time and food. Rev. J Biol Rhythms. 18, 250-260 (2003).

Sherman, H., Genzer, Y., Cohen, R., Chapnik, N., Mdar, Z. & Froy, O. Timed high-fat diet resets circadian metabolism and prevents obesity. FASBE J. 26, 3493-3502 (2012).

Shibata, S., Tahara, Y. & Hirao, A. The adjustment and manipulation of biological rhythms by light, nutrition, and abused drugs. Rev. Adv Drug Deliv. 62, 918-927 (2010).

Shimazu, S., Minami, A., Kusumoto, H. & Yoneda, F. Antidepressant-like effects of selegiline in the forced swim test. Eur Neuropsychopharmacol. 15, 563-571 (2005).

Stunkard, A. J., Grace, W. J. & Wolf, H. G. The night-eating syndrome; a pattern of food intake among certain obese patients.. Am J Med. 19, 78-86 (1955).

Suárez-Trujillo, A. & Casey, T. M. Serotoninergic and Circadian Systems: Driving Mammary Gland Development and Function. Front Physiol. 7, 301 (2016).

Sugimori, H., Yoshida, K. & Izuno, T. Analysis of factors that influence body mass index from ages 3 to 6 years: A study based on the Toyama cohort study. Pediatr Int. 46, 302-310 (2004).

Sullivan, E. L., Daniels, A. J., Koegler, F. H. & Cameron, J. L. Evidence in female rhesus monkeys (Macaca mulatta) that nighttime caloric intake is not associated with weight gain. Obes Res. 13, 2072-2080 (2005).

Szafarczyk, A., Ixart, G., Alonso, G., Malaval, F., Nouguier-Soule, J. & Assenmacher, I. Neural control of circadian rhythms in plasma ACTH, plasma corticosterone and motor activity. J Physiol. 77, 969-976 (1981).

Tahara, Y., Kuroda, H., Saito, K., Nakajima, Y., Kubo, Y., Ohnishi, N., Seo, Y., Otsuka, M., Fuse, Y., Ohura, Y., Komatsu, T., Moriya, Y., Okada, S., Furutani, N., Hirao, A., Horikawa, K., Kudo, T. & Shibata, S. In Vivo Monitoring of Peripheral Circadian Clocks in the Mouse. Current Biology. 22, 1029-1034 (2012).

Tahara, Y., Otsuka, M., Fuse, Y., Hirao, A. & Shibata, S. Refeeding after fasting elicits insulin-dependent regulation of Per2 and Rev-erbα with shifts in the liver clock. J Biol Rhythms. 26, 230-240 (2011).

Tahara, Y. & Shibata, S. Chronobiology and nutrition. Neuroscience. 253, 78-88 (2013).

Tahara, Y. & Shibata, S. Circadian rhythms of liver physiology and disease: experimental and clinical evidence. Nat Rev Gastroenterol Hepatol. 13, 217-226 (2016).

Tahara, Y., Shiraishi, T., Kikuchi, Y., Haraguchi, A., Kuriki, D., Sasaki, H., Motohashi, H., Sakai, T. & Shibata, S. Entrainment of the mouse circadian clock by sub-acute physical and psychological stress. Sci Rep. 5, 11417 (2015).

Takahashi, M., Haraguchi, A., Tahara, Y., Aoki, N., Fukazawa, M., Tanisawa, K., Ito, T., Nakaoka, T., Higuchi, M. & Shibata, S. Positive association between physical activity and PER3 expression in older adults. Sci Rep. 7, 39771 (2017).

Turek, F. W., Joshu, C., Kohsaka, A., Lin, E., Ivanova, G., McDearmon, E., Laposky, A., Losee-Olson, S., Easton, A., Jensen, D. R., Eckel, R. H., Takahashi, J. S. & Bass, J. Obesity and metabolic syndrome in circadian clock mutant mice. Science. 308, 1043-1045 (2005).

Ueda, H. R., Chen, W., Adachi, A., Wakamatsu, H., Hayashi, S., Takasugi, T., Nagano, M., Nakahama, K., Suzuki, Y., Sugano, S., Iino, M., Shigeyoshi, Y. & Hashimoto, S. A transcription factor response element for gene expression during circadian night. Nature. 418, 534-539 (2002).

Wang, X., Xue, J., Yang, J. & Xie, M. Timed high-fat diet in the evening affects the hepatic

circadian clock and PPARa-mediated lipogenic gene expressions in mice. Genes Nutr. 8, 457-463 (2013).

Watanabe, M., Hida, A., Kitamura, S., Enomoto, M., Ohsawa, Y., Katayose, Y., Nozaki, K., Moriguchi, Y., Aritake, S., Higuchi, S., Tamura, M., Kato, M. & Mishima, K. Rhythmic expression of circadian clock genes in human leukocytes and beard hair follicle cells. Biochem Biophys Res Commun. 425, 902-907 (2012).

Weaver, D. R. The suprachiasmatic nucleus: A 25-year retrospective. J Biol Rhythms. 13, 100-112 (1998).

Wehrens, S. M. T., Christou, S., Isherwood, C., Middleton, B., Gibbs, M. A., Archer, S. N., Skene, D. J. & Johnston, J. D. Meal Timing Regulates the Human Circadian System. Curr Biol. 27, 1768-1775 (2017).

Winkelman, J. W. Clinical and polysomnographic features of sleep-related eating disorder. J Clin Psychiatryii. 59, 14-19 (1998).

World Health Organization. Global Health Observatory (GHO) data. http://www.who.int/gho/ncd/risk_factors/overweight_text/en/. 18/11/2017 (2016).

World Health Organization. Investing in mental health: evidence for action. 6-7 (2013).

Wu, T., Sun, L., ZhuGe, F., Guo, X., Zhao, Z., Tang, R., Chen, Q., Chen, L., Kato, H. & Fu, Z. Differential roles of breakfast and supper in rats of a daily three-meal schedule upon circadian regulation and physiology. Chronobiol Int. 28, 890-903 (2011).

Yamada, J. & Sugimoto, Y. Differential effects of the 5-HT2 receptor antagonist on the anti-immobility effects of noradrenaline and serotonin reuptake inhibitors in the forced swimming test. Brain Res. 958, 161-165 (2002).

Yoo, S. H., Yamazaki, S., Lowrey, P. L., Shimomura, K., Ko, C. H., Buhr, E. D., Siepka, S. M., Hong, H. K., Oh, W. J., Yoo, O. J., Menaker, M. & Takahashi, J. S. PERIOD2::LUCIFERASE real-time reporting of circadian dynamics reveals persistent circadian oscillations in mouse peripheral tissues. Proc Natl Acad Sci U S A. 101, 5339-5346 (2003).

Zhang, S., Zeitzer, J. M., Yoshida, Y., Wisor, J. P., Nishino, S., Edgar, D. M. & Mignot, E. Lesions of the suprachiasmatic nucleus eliminate the daily rhythm of hypocretin-1 release. Sleep. 27, 619-627 (2004).

Zhang, X., Patel, S. P., McCarthy, J. J., Rabchevsky, A. G., Goldhamer, D. J. & Esser, K. A. A non-canonical E-box within the MyoD core enhancer is necessary for circadian expression in skeletal muscle. Nucleic Acids Res. 40, 3419-3430 (2012).

早稲田大学　博士（理学）　学位申請　研究業績書

氏 名　　原口 敦嗣　　印

（2018 年 1 月　現在）

種 類 別	題名、　発表・発行掲載誌名、　発表・発行年月、　連名者（申請者含む）
論文○	**Haraguchi, A.**, Fukuzawa, M., Iwami, S., Nishimura, Y., Motohashi, H., Tahara, Y. & Shibata, S. Night eating model shows time-specific depression-like behavior. Sci Rep. 8, 1081 (2018).
○	**Haraguchi, A.**, Aoki, N., Ohtsu, T., Ikeda, Y., Tahara, Y. & Shibata, S. Controlling access time to high fat diet during inactive period protects against obesity and abnormal phase-shift of peripheral clock in mice. Chronobiol Int. 31, 935-944 (2014).
	Tahara, Y., Yamazaki, M., Sukigara, H., Motohashi, H., Sasaki, H., Miyakawa, H., **Haraguchi, A.**, Ikeda, Y., Fukuda, S. & Shibata, S. Gut Microbiota-Derived Short Chain Fatty Acids Induce Circadian Clock Entrainment in Mouse Peripheral Tissue. Sci Rep. 8, 1395 (2018).
	Wada, M., Orihara, K., Kamagata, M., Hama, K., Sasaki, H., **Haraguchi, A.**, Miyakawa, H., Nakao, A. & Shibata, S. Circadian clock-dependent increase in salivary IgA secretion modulated by sympathetic receptor activation in mice. Sci Rep. 7, 8802 (2017).
	Motohashi, H., Sukigara, H., Tahara, Y., Saito, K., Yamazaki, M., Shiraishi, T., Kikuchi, Y., **Haraguchi, A.** & Shibata, S. Polyporus and Bupleuri radix effectively alter peripheral circadian clock phase acutely in male mice. Nutr Res. 43, 16-24 (2017).
	Shinozaki, A., Misawa, K., Ikeda, Y., **Haraguchi, A.**, Kamagata, M., Tahara, Y. & Shibata, S. Potent Effects of Flavonoid Nobiletin on Amplitude, Period, and Phase of the Circadian Clock Rhythm in PER2::LUCIFERASE Mouse Embryonic Fibroblasts. PLoS One. 12, e0170904 (2017).
	Tahara, Y., Takatsu, Y., Shiraishi, T., Kikuchi, Y., Yamazaki, M., Motohashi, H., Muto, A., Sasaki, H., **Haraguchi, A.**, Kuriki, D., Nakamura, T. J. & Shibata, S. Age-related circadian disorganization caused by sympathetic dysfunction in peripheral clock regulation. NPJ Aging Mech Dis. 3, 16030 (2017).
	Takahashi, M., **Haraguchi, A.**, Tahara, Y., Aoki, N., Fukazawa, M., Tanisawa, K., Ito, T., Nakaoka, T., Higuchi, M. & Shibata, S. Positive association between physical activity and PER3 expression in older adults. Sci Rep. 7, 39771 (2017).
	Fukuda, T., **Haraguchi, A.**, Kuwahara, M., Nakamura, K., Hamaguchi, Y., Ikeda, Y., Ishida, Y., Wang, G., Shirakawa, C., Tanihata, Y., Ohara, K. & Shibata, S. l-Ornithine affects peripheral clock gene expression in mice. Sci Rep. 6, 34665 (2016).
	Tahara, Y., Yokota, A., Shiraishi, T., Yamada, S., **Haraguchi, A.**, Shinozaki, A. & Shibata, S. In vitro and in vivo Phase Changes of the Mouse Circadian Clock by Oxidative Stress. *Journal of Circadian Rhythms*. 14, 1-7 (2016).
	Tanabe, K., Kitagawa, E., Wada, M., **Haraguchi, A.**, Orihara, K., Tahara, Y., Nakao, A. & Shibata, S. Antigen exposure in the late light period induces severe symptoms of food allergy in an OVA-allergic mouse model. Sci Rep. 5, 14424 (2015).
	Hamaguchi, Y., Tahara, Y., Kuroda, H., **Haraguchi, A.** & Shibata, S. Entrainment of mouse peripheral circadian clocks to <24 h feeding/fasting cycles under 24 h light/dark conditions. Sci Rep. 5, 14207 (2015).

早稲田大学　博士（理学）　学位申請　研究業績書

種 類 別	題名、　発表・発行掲載誌名、　発表・発行年月、　連名者（申請者含む）
論文	Tahara, Y., Shiraishi, T., Kikuchi, Y., **Haraguchi, A.**, Kuriki, D., Sasaki, H., Motohashi, H., Sakai, T. & Shibata, S. Entrainment of the mouse circadian clock by sub-acute physical and psychological stress. Sci Rep. 5, 11417 (2015). Ohnishi, N., Tahara, Y., Kuriki, D., **Haraguchi, A.** & Shibata, S. Warm water bath stimulates phase-shifts of the peripheral circadian clocks in PER2::LUCIFERASE mouse. PLoS One. 9, e100272 (2014).
総説	柴田 重信, 池田 祐子, **原口 敦嗣**. 食行動と概日リズム調節機構. 医薬ジャーナル. 株式会社 医薬ジャーナル社. 第 50 巻・第 6 号. 2014 年 6 月.
講演	**Haraguchi, A.**, Fukuzawa, M., Nishimura, Y., Motohashi, H., Iwami, S. & Shibata, S. Night eating syndrome's feeding pattern causes depression-like behavior with time-dependence by using a model mouse with night eating syndrome. the XV European Biological Rhythms Society Congress (EBRS 2017). P.27. Academic Medical Centre (Netherland). August 2017. **Haraguchi, A.**, Fukuzawa, M., Nishimura, Y., Motohashi, H., Iwami, S. & Shibata, S. Night eating syndrome's feeding pattern causes depression-like behavior depends on time by using a model mouse with night eating syndrome. 第 23 回日本時間生物学会学術大会. P094. 名古屋大学. 2016 年 11 月. **原口 敦嗣**, 高橋 将記, 依田 卓也, 細川 正人, 谷澤 薫平, 樋口 満, 竹山 春子, 柴田 重信. 毛包細胞を用いた時計遺伝子発現パターン解析. 第 3 回アクティブ・エイジング研究所シンポジウム～超高齢社会におけるパラダイムシフト～. アクティブ・エイジング研究所融合研究. 早稲田大学東伏見キャンパス 79 号館(東京). 2015 年 10 月. **Haraguchi, A.**, Nishimura, Y., Fukuzawa, M. & Shibata, S. Effect of social jetlag on rhythm of locomotor activity and biological clock using by social jetlag model mice. UCLA-Waseda University International Training Program 2015. student presentations (1). UCLA (USA). October 2015. **Haraguchi, A.**, Fukuzawa, M., Nishimura, Y., Shibata, S. & Shibata, S. A model mouse with night eating syndrome affects the metabolic energy homeostasis and the central monoamine/peripheral circadian clock system. The 2015 Cold Spring Harbor Asia Conference. Suzhou (China). October 2015. **原口 敦嗣**, 西村 裕太郎, 高橋 将記, 柴田重信. モデルマウスを用いた社会的時差ボケが体内時計や行動リズムに与える影響に関する検証. 第 26 回霧島神経薬理フォーラム. 一般演題 B-6. 霧島国際ホテル(鹿児島). 2015 年 8 月. **原口 敦嗣**, 西村 裕太郎, 柴田 重信. 食事時間帯と social jet lag. 日本睡眠学会第 40 回定期学術集会. シンポジウム 2-3. 栃木県総合文化センター. 2015 年 7 月. **Haraguchi, A.**, Shinozaki, A., Yokota, A. & Shibata, S. A model mouse with night eating syndrome affects the metabolic energy homeostasis and the peripheral clock. 第 20 回日本時間生物学会学術大会. P-74. 九州大学医学部 百年講堂(福岡). 2014 年 11 月.

早稲田大学　博士（理学）　学位申請　研究業績書

種 類 別	題名、　発表・発行掲載誌名、　発表・発行年月、　連名者（申請者含む）
講演	**Haraguchi, A.**, Aoki, N., Ohtsu, T., Ikeda, Y., Tahara, Y. & Shibata, S. Controlling access time to high fat diet during inactive period protects against obesity and abnormal phase-shift of peripheral clock in mice. SRBR 2014. P167. Montana (USA). June 2014. **原口 敦嗣**, 佐々木 裕之, 田原 優, 柴田 重信. 高脂肪食の摂食量および時間帯のマウス代謝リズムに対する作用. 第 91 回日本生理学会大会. 3P-099. 鹿児島大学. 2014 年 3 月. **原口 敦嗣**, 斎藤 恵祐, 阿部 真太郎, 中尾 洋一, 井上 真郷, 柴田 重信. 医療用漢方処方箋 100 種の時計遺伝子発現を指標とした多変量解析. 第 6 回生物学・化学・情報科学融合のための戦略的先進理工学研究基盤の形成支援事業シンポジウム. FBT-1223. 早稲田大学西早稲田キャンパス(東京). 2013 年 12 月. **原口 敦嗣**, 田原 優, 柴田 重信. in vivo 概日時計測定法と AAV ベクターによる二色同時発光測定系の構築. in vivo イメージングフォーラム 2013. コクヨホール(東京). 2013 年 9 月. **原口 敦嗣**, 青木 菜摘, 大津 定治, 柴田 重信. 高脂肪食の摂取時刻や摂取タイミングによる体重や脂肪率、末梢時計への影響. 第 67 回 日本栄養・食糧学会大会. 3K-03p. 名古屋大学. 2013 年 5 月. **原口 敦嗣**, 青木 菜摘, 大津 定治, 柴田 重信. 高脂肪食の摂取時刻や摂取タイミングによる体重や脂肪率、末梢時計への影響. 第 90 回日本生理学会大会. 3PK-186. タワーホール船堀(東京). 2013 年 3 月. **原口 敦嗣**, 青木 菜摘, 大津 定治, 浜口 雄太郎, 柴田 重信. 高脂肪食の摂食時刻・持続時間の体重や脂肪および末梢時計リズムへの影響. 第 19 回日本時間生物学会学術大会. P077. 北海道大学学術交流会館. 2012 年 9 月.